The H/D-exchange Kinetics of the Escherichia coli Co-chaperonin GroES Studied by 2D-NMR and DMSO-Quenched Exchange Methods.

ARTICLE *in* JOURNAL OF MOLECULAR BIOLOGY · APRIL 2013

Impact Factor: 4.33 · DOI: 10.1016/j.jmb.2013.04.008 · Source: PubMed

8 AUTHORS, INCLUDING:

Atsushi Mukaiyama
Institute for Molecular Science
19 PUBLICATIONS **246** CITATIONS
SEE PROFILE

Tapan Chaudhuri
Indian Institute of Technology Delhi
40 PUBLICATIONS **750** CITATIONS
SEE PROFILE

Koichi Kato
Institute for Molecular Science
275 PUBLICATIONS **5,382** CITATIONS
SEE PROFILE

Kunihiro Kuwajima
The University of Tokyo
157 PUBLICATIONS **7,605** CITATIONS
SEE PROFILE

jmb Article

The H/D-Exchange Kinetics of the *Escherichia coli* Co-Chaperonin GroES Studied by 2D NMR and DMSO-Quenched Exchange Methods

Mahesh S. Chandak[1,2], Takashi Nakamura[1], Koki Makabe[1,2], Toshio Takenaka[1], Atsushi Mukaiyama[1], Tapan K. Chaudhuri[1,3], Koichi Kato[1,2] and Kunihiro Kuwajima[1,2]

1 - Okazaki Institute for Integrative Bioscience and Institute for Molecular Science, *National Institutes of Natural Sciences, 5-1 Higashiyama, Myodaiji, Okazaki 444-8787, Japan*

2 - Department of Functional Molecular Science, *School of Physical Sciences, The Graduate University for Advanced Studies (Sokendai), 5-1 Higashiyama, Myodaiji, Okazaki 444-8787, Japan*

3 - School of Biological Sciences, *Indian Institute of Technology Delhi, Hauz Khas, New Delhi 110016, India*

Correspondence to Kunihiro Kuwajima: *The Center for the Promotion of Integrated Sciences, the Graduate University for Advanced Studies (Sokendai), Shonan Village, Hayama, Kanagawa 240-0193, Japan. kuwajima@ims.ac.jp*

http://dx.doi.org/10.1016/j.jmb.2013.04.008

Edited by J. Clarke

Abstract

We studied hydrogen/deuterium-exchange reactions of peptide amide protons of GroES using two different techniques: (1) two-dimensional $^{1}H–^{15}N$ transverse-optimized NMR spectroscopy and (2) the dimethylsulfoxide-quenched hydrogen-exchange method combined with conventional $^{1}H–^{15}N$ heteronuclear single quantum coherence spectroscopy. By using these techniques together with direct heteronuclear single quantum coherence experiments, we quantitatively evaluated the exchange rates for 33 out of the 94 peptide amide protons of GroES and their protection factors, and for the remaining 61 residues, we obtained the lower limits of the exchange rates. The protection factors of the most highly protected amide protons were on the order of 10^{6}–10^{7}, and the values were comparable in magnitude to those observed in typical small globular proteins, but the number of the highly protected amide protons with a protection factor larger than 10^{6} was only 10, significantly smaller than the numbers reported for the small globular proteins, indicating that significant portions of free heptameric GroES are flexible and natively unfolded. The highly protected amino acid residues with a protection factor larger than 10^{5} were mainly located in three β-strands that form the hydrophobic core of GroES, while the residues in a mobile loop (residues 17–34) were not highly protected. The protection factors of the most highly protected amide protons were orders of magnitude larger than the value expected from the equilibrium unfolding parameters previously reported, strongly suggesting that the equilibrium unfolding of GroES is more complicated than a simple two-state or three-state mechanism and may involve more than a single intermediate.

Introduction

The *Escherichia coli* co-chaperonin GroES is a heptameric protein supermolecular assembly with a molecular weight of 73,000, and it forms a chaperonin complex with GroEL, which is a tetradecameric protein assembly with a molecular weight of 800,000.[1–3] The chaperonin complex is a dynamic molecular machine that mediates the folding reactions of various proteins in the bacterial cell in an ATP-dependent manner. Although a large number of biophysical and biochemical studies on the molecular mechanisms of the chaperonin function have been reported,[1–21] rather little is known about dynamic aspects and structural fluctuations of GroES, GroEL, and the related complexes. Structural fluctuations of GroES and GroEL are definitely important for formation of the chaperonin complex, recognition of substrate proteins by the complex, and chaperonin cycling of the GroEL/GroES

complex.[22–30] The large molecular weights of GroES, GroEL, and the chaperonin complex make it infeasible to study the structural fluctuations of these protein supermolecular assemblies by a hydrogen/deuterium (H/D)-exchange technique combined with conventional two-dimensional (2D) NMR spectroscopy. Therefore, there were no H/D-exchange studies of these protein assemblies in the native state until, in a very recent report, Zhang *et al.*[31] described nucleotide-induced conformational changes of GroEL mapped by H/D exchange monitored by Fourier transform ion cyclotron resonance mass spectrometry combined with limited proteolysis and high-performance liquid chromatography analysis, a technique useful for studying large proteins.

For GroES, however, the monomeric molecular weight is only 10,000, and hence, we can employ the following two techniques to obtain the well-resolved NMR spectra required for the H/D-exchange measurements of individual amide protons: (1) 2D $^{1}H–^{15}N$ transverse relaxation optimized spectroscopy (TROSY)[32,33] and (2) the dimethylsulfoxide (DMSO)-quenched H/D exchange (DMSO-QHX) method combined with $^{1}H–^{15}N$ heteronuclear single quantum coherence (HSQC) spectroscopy.[34,35] The TROSY technique, in combination with perdeuteration of protein, has opened avenues to the study of large proteins and protein assemblies with molecular weights larger than 50,000 by solution NMR,[32,33] and the technique was successfully applied for the NMR analysis of GroES and the GroEL/GroES complex, in which only the GroES portion was uniformly ^{15}N-labeled.[36,37] The DMSO-QHX method, first introduced by the Roder group,[34] is a very versatile method to characterize the H/D-exchange behaviors of proteins and protein assemblies, and the advantage of this method is twofold: (1) DMSO is a strong protein denaturant that can be used as a solubilizer of water-insoluble protein aggregates, and (2) the chemical exchange rates of peptide amide protons are substantially reduced in a DMSO solution (most typically 95% DMSO-d_6/5% D_2O, pH* 5.0), making it possible to observe the 2D NMR spectra of denatured monomeric proteins in the DMSO solution; pH* indicates the pH-meter reading. The DMSO-QHX method has thus been used widely for studying the H/D-exchange behaviors of various amyloid fibrils[35,38–44] and other protein supermolecular assemblies,[45,46] and it should be useful for studying the H/D-exchange behavior of GroES. The DMSO-QHX method was recently improved by Chandak *et al.*[47] by the use of spin desalting columns for medium exchange from D_2O to the DMSO solution.

The X-ray crystallographic structures of heptameric GroES and the GroEL/GroES/nucleotide complexes have been reported,[26,48–50] and the Protein Data Bank (PDB) coordinates are available for the complexes (PDB codes: 1AON, 1PCQ, 1PF9, 1SVT, and 1SX4). The GroES heptamer has a dome-like structure, approximately 75 Å in diameter and 30 Å high, with an 8-Å orifice in the center of its roof. The structure of each subunit is composed of an irregular β-barrel formed by five β-strands (strands B, C, D, E, and F), several reverse turns, a short 3_{10}-helix (residues 87–91), the N- and C-terminal β-strands (strands A and G) located at the subunit–subunit interface, and two loop regions, a flexible mobile loop (residues 17–34) and a roof hairpin loop (residues 44–58) (Fig. 1). The mobile loop of stand-alone GroES is natively unfolded as indicated by one-dimensional and 2D NMR spectra[22] and the reported crystal structure of GroES,[48] in which the mobile loop segment was disordered in six out of the seven subunits. The flexible nature of the mobile loop is crucial for the recognition by GroEL,[22–25] and the loop becomes structured upon interacting with GroEL.[49] Except for the mobile loop region, the GroES structure of the GroEL/GroES complexes is very similar to the structure of stand-alone GroES.[49] In spite of these unique structural characteristics of GroES, the unfolding transitions of GroES induced by denaturants and by increasing temperature are fully reversible[52–57] and often interpreted in terms of a simple two-state model of the unfolding accompanied by dissociation from the heptameric native state to the monomeric unfolded state.

Here, we studied the H/D-exchange reactions of free heptameric GroES by the TROSY technique and the DMSO-QHX technique combined with 2D $^{1}H–^{15}N$ HSQC spectra measured at a ^{1}H resonance frequency of 920 MHz. We quantitatively evaluated the apparent rate constants (k_{ex}) of H/D exchange for 33 out of the 94 peptide amide protons of GroES and their protection factors (P_f), and for the remaining 61 residues, we obtained the lower and the upper limits of the k_{ex} and P_f values, respectively. We show that the P_f values (10^6–10^7) of the most highly protected amide protons are comparable in magnitude to those observed in typical small globular proteins but that the number of the highly protected amide protons ($P_f > 10^6$) is significantly smaller than those reported for the small globular proteins, indicating that significant portions of GroES are flexible and natively unfolded. The flexible regions with weakly protected amide protons ($P_f < 10^4$) were mostly located in the mobile loop of residues 17–34, a reverse turn 49–52 at the top of the roof hairpin, and the region (strand E and the adjacent turns) between strands D and F (Fig. 1). Considering the oligomeric nature and physiological concentrations (~35 μM in monomer units)[58–60] of GroES and the P_f values of the most highly protected amide protons, the effective thermodynamic stability of GroES is well designed so as to be comparable to the stability of the small globular proteins. The P_f values of the

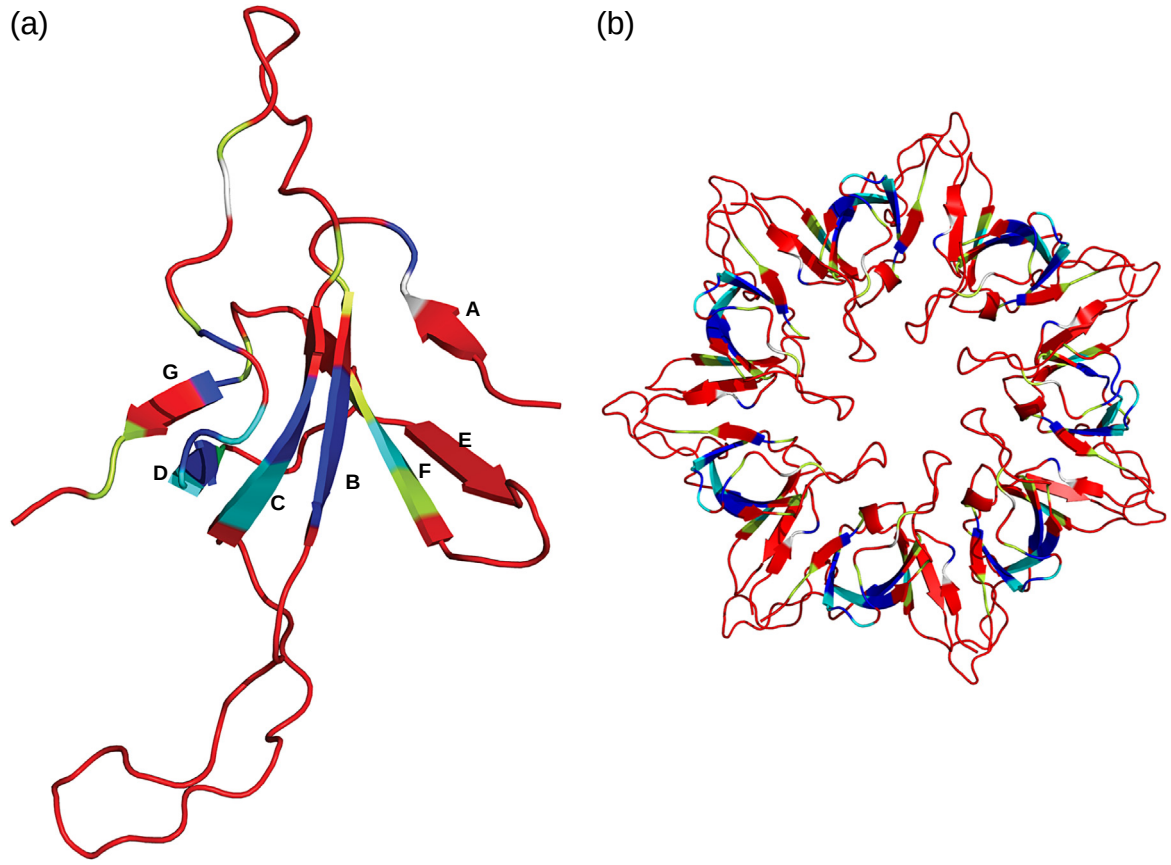

Fig. 1. The backbone structure of the GroES monomer unit (a) and the heptameric complex (b). The GroES portion of the GroEL/GroES/ADP complex (PDB code: 1AON) is shown. The backbone structure was analyzed by the method of Kabsch and Sander[51] using the DSSP program (http://swift.cmbi.ru.nl/gv/dssp/). The seven β-strands thus identified are labeled as A, B, C, D, E, F, and G in the order from the N-terminal to the C-terminal side in (a). The structure is classified by different colors according to the P_f values (red for $P_f < 10^4$, yellow for $10^4 \leq P_f < 10^5$, cyan for $10^5 \leq P_f < 10^6$, and blue for $10^6 \leq P_f$). The residues for which only the upper limits of P_f are known (sticks and plus marks in Fig. 8) are also shown in red. Two prolyl residues, Pro5 and Pro56, are shown in white. The figures were prepared using PyMOL (DeLano Scientific).

most highly protected amide protons were, however, a few orders of magnitude larger than those expected from the equilibrium unfolding parameters previously reported, strongly suggesting that the equilibrium unfolding of GroES is more complicated than a simple two-state or three-state mechanism and may involve more than a single intermediate.

Results

NMR spectra of GroES

The molecular weight (M_w = 73,000) of a free GroES heptamer is too large to obtain well-resolved NMR signals in conventional $^1H–^{15}N$ HSQC spectra of the protein. Figure 2a shows an HSQC spectrum of uniformly ^{15}N-labeled GroES in 90% H_2O/10% D_2O at pH 6.5 and 25 °C; as shown in the figure, we observed only 20 out of 94 expected peptide amide $^1H–^{15}N$ cross-peaks, with the observed cross-peaks belonging to the residue (Ala97) at the C terminus, residue 51 (Asn), and residues 17–34, which form a flexible mobile loop in the native state.[22,48] To overcome the problem of these poor NMR signals, we employed two different techniques, that is, (1) 2D $^1H–^{15}N$ TROSY[32,33] at a ^1H resonance frequency of 920 MHz and (2) the DMSO-QHX technique combined with conventional $^1H–^{15}N$ HSQC spectroscopy.[34,47]

Although the long recording time (~2.5 h) required in the TROSY experiment precludes measurements of fast-exchanging amide-proton signals by TROSY, we can use the assignments of the amide-proton signals of GroES, previously reported by Fiaux *et al.* (BioMagResBank entry 7091).[36] Figure 2b shows a TROSY spectrum of ^{15}N-labeled and perdeuterated GroES in 90% H_2O/10% D_2O at pH 6.5 and 25 °C. We observed essentially all peptide amide cross-peaks of GroES, and the assignments for the 89 cross-peaks previously reported are shown in Fig. 2b.

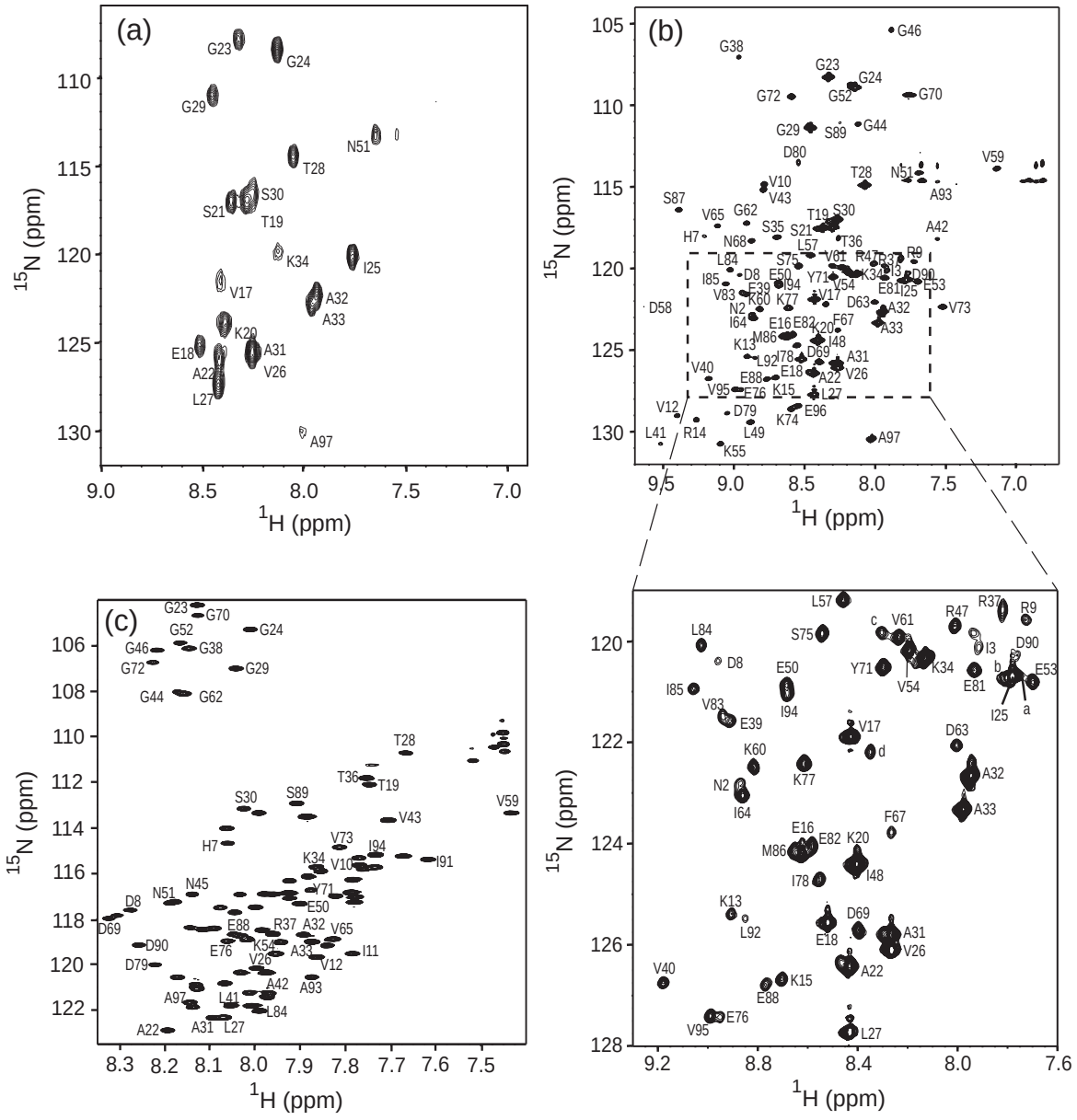

Fig. 2. 2D NMR spectra of GroES. (a) A ^{1}H 500-MHz [^{15}N, ^{1}H]-HSQC spectrum of uniformly ^{15}N-labeled native GroES in 90% H_2O/10% D_2O at pH 6.5 and 25 °C. (b) A ^{1}H 920-MHz [^{15}N, ^{1}H]-TROSY-HSQC spectrum of {D, ^{15}N}-labeled native GroES in 90% H_2O/10% D_2O at pH 6.5 and 25 °C. The crowded region enclosed by a broken framed rectangle is expanded under the main panel. The cross-peaks labeled by a, b, c, and d indicate four unidentified amide protons. (c) A ^{1}H 920-MHz [^{15}N, ^{1}H]-HSQC spectrum of uniformly ^{15}N-labeled unfolded GroES in the DMSO solution (95% DMSO-d_6/5% D_2O, pH* 5.0) at 25 °C.

The DMSO-QHX method is useful for measurements of the H/D exchange of a protein supermolecular assembly, and the DMSO solution (95% DMSO-d_6/5% D_2O, pH* 5.0), which is used to quench the H/D-exchange reactions, effectively dissociates the GroES heptamer to unfolded monomers, making it possible to obtain well-resolved HSQC spectra of unfolded monomeric GroES. However, we have to assign the HSQC cross-peaks of GroES in the DMSO solution. The backbone assignments of {^{13}C, ^{15}N}-double labeled GroES in the DMSO solution were thus obtained by three-dimensional CBCACONH and HNCACB experiments recorded on a 920-MHz NMR instrument. We obtained assignments of 46 out of the 94 backbone amide protons, and Fig. 2c shows a ^{1}H–^{15}N HSQC spectrum of GroES in the DMSO solution (Fig. 2c).

H/D-exchange kinetics of GroES

Changes in the NMR spectra during H/D-exchange reactions

The H/D-exchange reaction of the protein was started by 10-fold dilution of 3 mM (0.43 mM as the heptamer) ^{15}N-labeled GroES in 25 mM phosphate buffer in H_2O at pH 6.5 into 25 mM phosphate buffer in D_2O at pH* 6.5 at 25.0 °C, and the reactions of the amide protons were directly monitored by the ^{1}H–^{15}N TROSY HSQC spectra. Figure 3 shows typical spectra observed at different exchange times, 4.6, 27.4, and 161.9 h. Because the first time point, which included a half of the recording time and a time required for adjustment of the NMR spectrometer, was already 4.6 h after starting the H/D exchange, we could monitor only slowly exchanging amide protons in the TROSY experiments. Interestingly, however, we observed all the amide-proton signals of residues 17–34 and residues 51–53. Residues 17–34 are in the mobile loop region, and residues 51–53 are located at the top of a roof hairpin loop.[22,48] These residues were not highly protected, as indicated by the DMSO-QHX as well as direct HSQC H/D-exchange experiments (see below). Because the solution contained 10% H_2O, these protons in the flexible regions exhibited significant signal intensities in spite of the H/D exchange of the amide protons already saturated at the first time point (4.6 h). To distinguish between such fast-exchanging amide protons in flexible regions and very slowly exchanging amide protons that did not show any significant change in signal intensity during the H/D-exchange measurement, we carried out the same H/D-exchange experiment at a higher pH (pH* 7.5), where the intrinsic chemical exchange rates of the amide protons were increased by 10 times.[61,62] As a result, we identified 27 slowly exchanging amide protons. These 27 amide protons consisted of those of Arg9, Gly38, Glu39, Gly44, Leu49, Lys55, Val59, Lys60, Gly62, Ile64, Phe67, Val83, Leu84, Ile85, Asp90, Ile94, and Val95, for which we observed significant exchange decay kinetics at pH* 6.5, and those of Val12, Lys13, Val40, Leu41, Asp63, Val65, and four as-yet-unidentified residues, for which we observed clear decay kinetics at pH* 7.5. The cross-peaks of these residues are labeled by a one-letter amino acid code plus a residue number in blue in Fig. 3a; the four unidentified cross-peaks are labeled as a, b, c, and d in the order of the ^{1}H chemical shift. The chemical shifts of cross-peak a were coincident with those of the Ile25 cross-peak, and the observed cross-peak appeared as a composite of two components with very different line widths (inset of Fig. 3a). For the remaining 67 fast-exchanging amide protons, we could not observe the exchange kinetics by TROSY, and the rate constant, k_{ex}, values of the H/D-

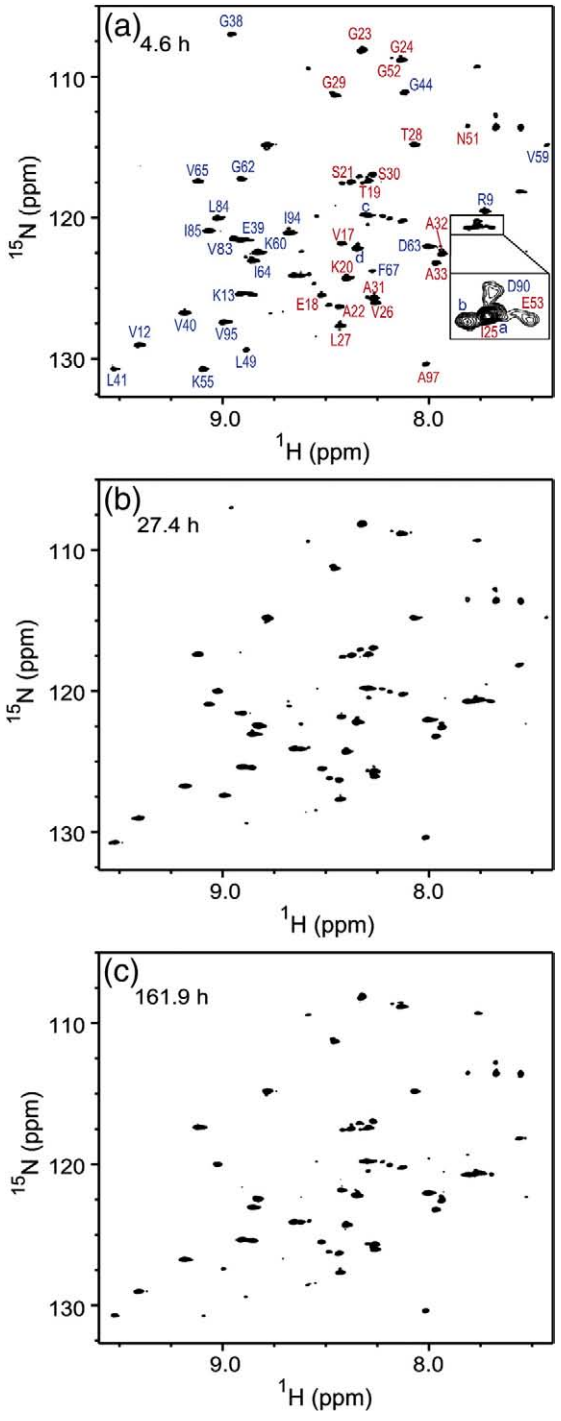

Fig. 3. [^{15}N, ^{1}H]-TROSY-HSQC spectra of {D, ^{15}N}-labeled GroES in 90% D_2O/10% H_2O at pH* 6.5 and 25 ºC at different H/D-exchange times. The H/D-exchange times are as follows: (a) 4.6 h, (b) 27.4 h, and (c) 161.9 h. The amino acid residues shown by the one-letter amino acid code plus residue number in blue indicate slowly exchanging amide protons, while those in red indicate fast-exchanging amide protons with significant signal intensities. The four unidentified cross-peaks are labeled as a, b, c, and d. All spectra were processed with identical parameters and shown with the same contour levels.

exchange reactions were estimated to be larger than 0.0002 (=3/(4.6 × 60 × 60)) s^{-1}, because more than 95% of the signal intensity change occurred at the first time point (4.6 h).

In the DMSO-QHX experiments, the H/D-exchange reaction of the protein was also started by 10-fold dilution of 3 mM ^{15}N-labeled GroES in H_2O at pH 6.5 into the D_2O buffer solution at pH* 6.5 at 25.0 °C. At each predetermined exchange time, 1.0 mL of the reaction mixture pre-dispensed in a microtube was taken, the reaction was quenched in liquid nitrogen, and the frozen mixture was kept in a freezer at −85 °C until the medium exchange and the subsequent NMR measurement. For the NMR measurement, the frozen sample was thawed at room temperature, the medium containing 90% D_2O/10% H_2O was exchanged for the DMSO solution by using a spin desalting column,[47] and the ^{1}H–^{15}N HSQC spectrum of the protein was measured. The first time point available in the DMSO-QHX reaction was 20 min, and we measured the exchange reaction until 10 days after starting the H/D exchange. Moreover, in the DMSO-QHX experiment, we could also obtain the spectrum with no H/D exchange (Fig. 2c), that is, at zero time of the H/D exchange, under the initial H/D-exchange condition by carrying out the medium exchange of the protein solution in H_2O for the DMSO solution. Figure 4 shows ^{1}H–^{15}N HSQC spectra of the protein obtained by the DMSO-QHX method with different exchange times, 20 min and 10 days (Fig. 4a and b), after starting the H/D exchange under the H/D-exchange condition (90% D_2O/10% H_2O, pH* 6.5), and with complete exchange by heating the sample under the exchange condition at 70 °C for 30 min (Fig. 4c). We obtained the k_{ex} values of 15 amide protons, and the remaining 31 of the 46 assigned amide protons were too fast to measure by DMSO-QHX, and the k_{ex} values of these fast-exchanging protons were estimated to be larger than 0.0025 (=3/(20 × 60)) s^{-1}, since more than 95% of the signal intensity change occurred at the first time point (20 min).

We also measured the 18 amide-proton cross-peaks [residues 17–33, and residue 51 (Asn)], which were observed by the direct ^{1}H–^{15}N HSQC spectra of native GroES (Fig. 2a), at different exchange times in 90% D_2O/10% H_2O at pH* 6.5 and 25 °C. However, at the first time point (16 min) after starting the H/D exchange, all these amide protons, except for those of Ser21 and Ile25, were almost fully (approximately more than 90%) exchanged out, indicating that the k_{ex} values of the H/D-exchange reactions were larger than 0.002 s^{-1} (=2.3/(16 × 60)) s^{-1}), since more than 90% of the signal intensity change occurred at 16 min.

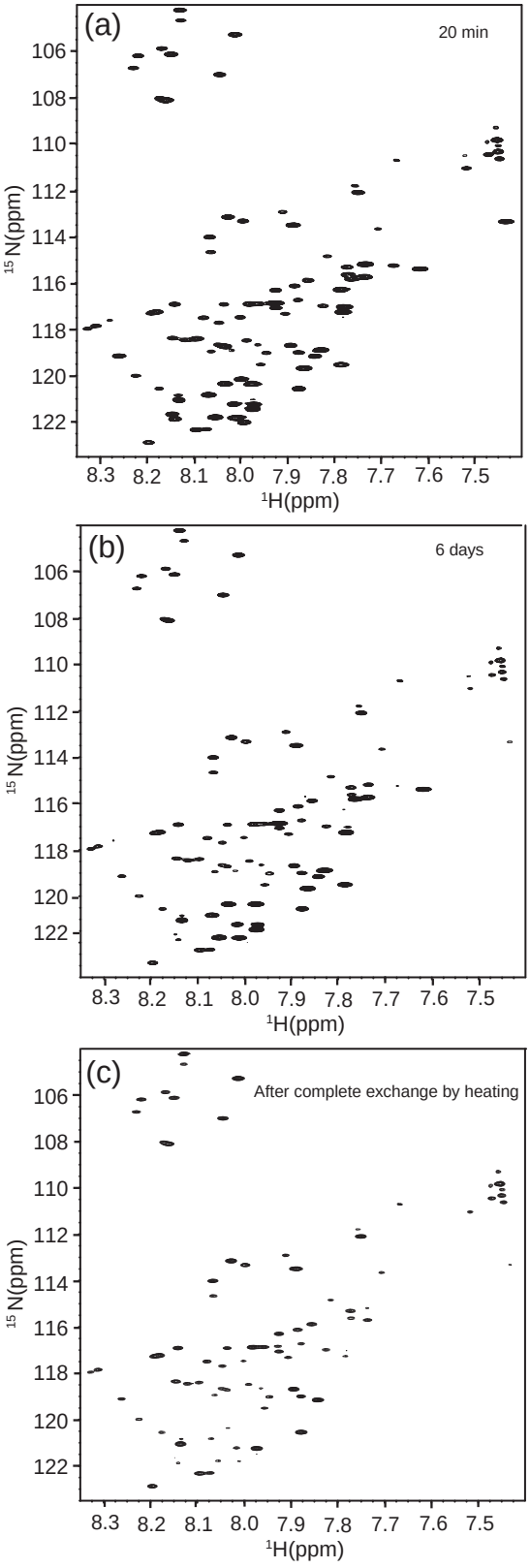

Fig. 4. (a) [^{15}N, ^{1}H]-HSQC spectra of ^{15}N-labeled unfolded GroES in the DMSO solution at 25 °C with different H/D-exchange times under the H/D-exchange condition (pH* 6.5 and 25 °C), 20 min (a), 6 days (b). The spectrum in (c) is that after complete H/D exchange by heating at 70 °C for 30 min under the H/D-exchange condition.

Kinetic progress curves of H/D exchange

We observed H/D-exchange kinetics for 27 slowly exchanging amide protons, including the 4 unidentified very slowly exchanging protons by TROSY, 15 amide protons by DMSO-QHX, and 2 amide protons by direct HSQC. Among these amide protons, the exchange reactions of the protons of 7 residues (Gly38, Gly44, Val59, Gly62, Leu84, Asp90, and Ile94) were measured by both TROSY and DMSO-QHX at pH* 6.5. All the H/D-exchange kinetics observed were single exponential, and the kinetics measured by TROSY were coincident with those measured by DMSO-QHX except for the kinetics of the Ile94 amide proton, for which the observed H/D-exchange rate constant ($k_{ex} = 2.9 \times 10^{-5}$ s^{-1}) by TROSY was 6 times larger than the rate constant ($k_{ex} = 0.45 \times 10^{-5}$ s^{-1}) measured by DMSO-QHX.

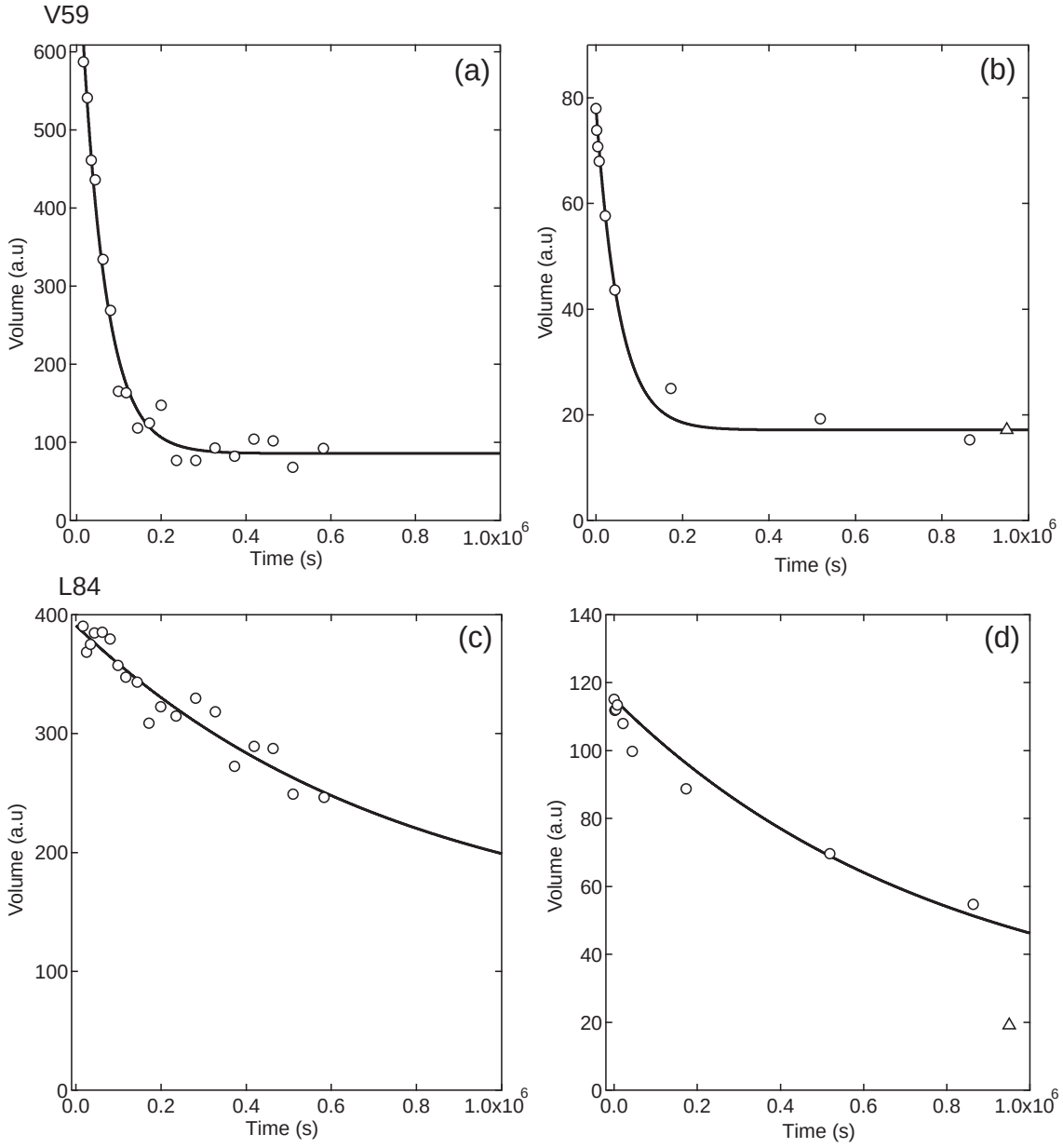

Fig. 5. Kinetic progress curves of the H/D-exchange reactions of GroES monitored by TROSY [(a) and (c)] and DMSO-QHX [(b) and (d)] (pH* 6.5 and 25°). (a) and (b) indicate the H/D-exchange curves of the Val59 amide proton, and (c) and (d) indicate the H/D-exchange curves of the Leu84 amide proton. Open triangles in (b) and (d) indicate the peak volumes after complete H/D exchange. The thick continuous lines are the theoretical exchange curves fitted to a single-exponential function [Eq. (13)] with k_{ex} values of 1.7×10^{-5} s^{-1} (a), 1.9×10^{-5} s^{-1} (b), 0.9×10^{-6} s^{-1} (c), and 1.3×10^{-6} s^{-1} (d).

The discrepancy in k_{ex} between TROSY and DMSO-QHX remains to be solved, but we employed the value obtained by DMSO-QHX, since our assignment of the Ile94 amide proton in the HSQC spectrum of GroES in the DMSO solution was quite straightforward.

Figure 5 shows typical kinetic progress curves of the H/D-exchange reactions of GroES monitored by TROSY and DMSO-QHX. The exchange curve of the Val59 amide proton measured by TROSY showed a single-exponential decay with a k_{ex} of 1.7×10^{-5} s^{-1} (Fig. 5a), and this was coincident with the exchange curve measured by DMSO-QHX, which gave a k_{ex} of 1.9×10^{-5} s^{-1} (Fig. 5b). Similarly, the exchange curve of Leu84 measured by TROSY gave a k_{ex} of 0.9×10^{-6} s^{-1} (Fig. 5c), which was coincident with the exchange curve measured by DMSO-QHX, which gave a k_{ex} of 1.3×10^{-6} s^{-1} (Fig. 5d). Figure 6 shows a typical H/D-exchange curve of the fast-exchanging amide proton of Ser21 monitored by direct HSQC. The exchange curve was single exponential, and the k_{ex} value was 0.0014 s^{-1}.

Table 1 summarizes the k_{ex} values of peptide amide protons measured at pH* 6.5 in the present study, and the k_{ex} values of very slowly exchanging amide protons measured at pH* 7.5 are summarized in Table 2. We obtained the k_{ex} values at pH* 6.5 for 28 out of the 94 expected amide protons by either TROSY, DMSO-QHX, or direct HSQC. For very slowly exchanging amide protons of five residues (Lys13, Val40, Asp63, and the two unidentified residues labeled as a and c in Fig. 3a), we obtained the k_{ex} values only by TROSY at pH* 7.5; cross-peaks b and d in Fig. 3a were assigned to the amide protons of Ile11 and Ile91 whose exchange rates were also measured at pH* 6.5 by DMSO-QHX (see below). For all the other amide protons, the H/D-exchange rates were too fast to monitor by TROSY, DMSO-QHX, or direct HSQC. Therefore, for these 61 fast-exchanging amide protons, the lower limits of k_{ex} are shown in Table 1. The lower limits were as follows: $\log(k_{ex}/s^{-1}) > -3.7$ for the amide protons monitored by TROSY, $\log(k_{ex}/s^{-1}) > -2.6$ for those monitored by DMSO-QHX, and $\log(k_{ex}/s^{-1}) > -2.6$ for those monitored by direct HSQC.

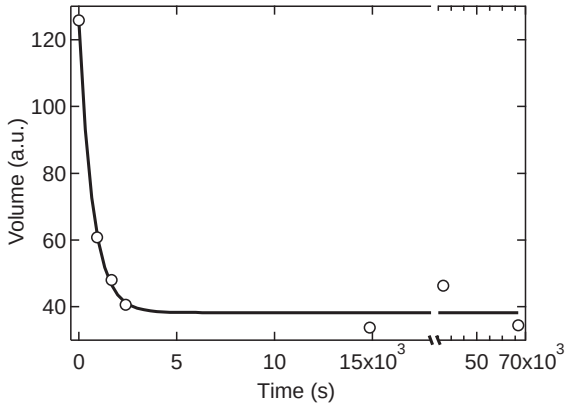

Fig. 6. A typical kinetic progress curve of the H/D-exchange reaction of the Ser21 amide proton monitored by direct HSQC (pH* 6.5 and 25 °C). The thick continuous line is the theoretical exchange curve fitted to a single-exponential function with a k_{ex} of 0.0014 s^{-1} [Eq. (13)].

H/D-exchange progress curves of unidentified amide protons

Figure 7 shows H/D-exchange progress curves of the four unidentified and very slowly exchanging amide protons, which are labeled as a, b, c, and d in Fig. 3a, measured by TROSY at pH* 7.5 and 25 °C. The k_{ex} values for these protons obtained by fitting to a single-exponential function were 6.2×10^{-7}, 8.5×10^{-7}, 6.3×10^{-7}, and 1.1×10^{-6} s^{-1} for cross-peaks a, b, c, and d, respectively. For cross-peak a, which appeared as a composite peak of the very slowly exchanging amide proton and the fast-exchanging Ile25 proton, we used the difference in the peak volume to extract solely the volume of the very slowly exchanging component (see the inset of Fig. 7a). There were five amino acid residues (Leu6, Ile11, Asn45, Ile66, and Ile91) whose amide-proton cross-peaks were not yet identified in the TROSY spectrum,[36] and among these five residues, three residues, Ile11, Asn45, and Ile91, had the cross-peaks identified in the HSQC spectrum of unfolded monomeric GroES in the DMSO solution (Fig. 2c). The k_{ex} values for these three residues were thus determined by DMSO-QHX, and they were 2.4×10^{-7}, 0.0018, and 1.7×10^{-7} s^{-1} for Ile11, Asn45, and Ile91, respectively, at pH* 6.5. The H/D-exchange rate at pH* 7.5 is expected to be 10-fold higher than that at pH* 6.5, and hence the expected k_{ex} values at pH* 7.5 are 2.4×10^{-6}, 0.018, and 1.7×10^{-6} s^{-1} for Ile11, Asn45, and Ile91, respectively. Apparently, the k_{ex} (0.018 s^{-1}) for Asn45 is too fast to measure by TROSY, but those for Ile11 and Ile91 are very close to the measured values of cross-peaks d and b, respectively, at pH* 7.5. We thus assigned cross-peaks d and b to the amide protons of Ile11 and Ile91, respectively. The remaining two cross-peaks (a and c) were thus assigned to the amide protons of Leu6 and Ile66. Because the k_{ex} values of cross-peaks a and c were essentially identical, the k_{ex} values for the two residues were assumed to be 6.2×10^{-7} s^{-1} by taking an average of the values for cross-peaks a and c. The k_{ex} values thus estimated for Leu6, Ile11, Ile66, and Ile91 are also included in Table 2.

Protection profile

The protection factor, P_f, of each amide proton of the protein is given by a ratio of the rate constant, k_{int},

Table 1. H/D-exchange parameters of GroES at pH* 6.5 and 25 °C

Residue	k_{int} (s^{-1})	log(k_{ex}/s^{-1})	log P_f	Methods[a]
N2	2.76×10^2	>−3.74[b]	<6.18[b]	T
I3	0.842	>−3.74	<3.67	T
R4	1.53	>−3.74	<3.93	T
P5	—	—	—	—
L6	0.328	n.a.	n.a.	
H7	2.50	>−2.60	<3.00	D
D8	2.92	>−2.60	<3.07	D
R9	1.73	−4.55	4.79	T
V10	0.717	−3.34	3.20	D
I11	0.293	−6.62	6.08	D
V12	0.255	−6.43	5.83	D
K13	1.43	<−6.77[c]	>6.92[c]	T
R14	3.43	>−3.74	<4.28	T
K15	3.27	>−3.74	<4.26	T
E16	0.888	>−3.74	<3.69	T
V17	0.308	>−3.74	<3.23	T
E18	0.488	>−2.62	<2.31	H
T19	1.31	>−2.60	<2.72	D
K20	3.13	>−2.60	<3.10	D
S21	6.68	−2.85	3.68	H
A22	4.32	>−2.60	<3.24	D
G23	4.03	>−2.60	<3.21	D
G24	5.96	>−2.60	<3.38	D
I25	0.596	−2.85	2.62	H
V26	0.255	>−2.60	<2.01	D
L27	0.413	>−2.60	<2.22	D
T28	1.14	>−2.60	<2.66	D
G29	6.38	>−2.60	<3.41	D
S30	7.50	>−2.60	<3.48	D
A31	4.32	>−2.60	<3.24	D
A32	2.16	>−2.62	<2.95	H
A33	2.16	>−2.60	<2.94	D
K34	1.97	>−2.60	<2.90	D
S35	6.68	>−3.74	<4.57	T
T36	3.67	>−2.60	<3.17	D
R37	4.12	>−2.60	<3.22	D
G38	6.68	−4.84	5.67	T, D
E39	0.996	−5.35	5.34	T
V40	0.308	<−6.77	>6.25	T
L41	0.413	−6.42	6.04	D
A42	1.33	−3.75	3.88	D
V43	0.432	>−2.60	<2.24	D
G44	2.92	−4.25	4.72	T, D
N45	9.89	>−2.60	<3.60	D
G46	8.41	>−3.74	<4.67	T
R47	3.85	>−3.74	<4.33	T
I48	0.669	>−3.74	<3.57	T
L49	0.336	−3.94	3.46	T
E50	0.416	>−2.60	<2.22	D
N51	4.76	>−2.60	<3.28	D
G52	8.41	>−3.74	<4.67	T
E53	0.996	>−3.74	<3.74	T
V54	0.308	>−3.74	<3.23	T
K55	1.43	−4.23	4.39	T
P56	—	—	—	—
L57	0.328	>−3.74	<3.26	T
D58	0.675	>−3.74	<3.57	T
V59	0.288	−4.75	4.21	T, D
K60	1.43	−6.32	6.47	T
V61	0.570	>−3.74	<3.50	T
G62	2.92	−4.63	5.09	T, D
D63	1.62	<−6.77	>6.98	T
I64	0.269	−6.52	5.95	T
V65	0.255	−6.70	6.10	D
I66	0.293	n.a.	n.a.	
F67	0.734	−4.14	4.01	T
N68	7.67	>−3.74	<4.63	T
D69	2.29	>−2.60	<2.96	D
G70	2.68	>−2.60	<3.03	D
Y71	1.72	>−2.60	<3.83	D
G72	4.52	>−2.60	<3.25	D
V73	0.639	>−2.60	<2.40	D
K74	1.43	>−3.74	<3.90	T
S75	6.68	>−3.74	<4.57	T
E76	1.34	>−2.60	<2.73	D
K77	1.40	>−3.74	<3.89	T
I78	0.532	>−3.74	<3.47	T
D79	0.645	>−2.60	<2.41	D
N80	4.45	>−3.74	<4.39	T
E81	1.41	>−3.74	<3.89	T
E82	0.479	>−3.74	<3.42	T
V83	0.308	−4.69	4.18	T
L84	0.413	−5.97	5.59	T, D
I85	0.249	−5.25	4.65	T
M86	1.25	>−3.74	<3.84	T
S87	6.53	>−3.74	<4.56	T
E88	1.34	−3.11	3.24	D
S89	3.61	>−2.60	<3.16	D
D90	2.18	−4.49	4.83	D
I91	0.269	−6.76	6.19	D
L92	0.336	>−3.74	<3.27	T
A93	1.33	−3.50	3.62	D
I94	0.403	−5.34	4.95	D
V95	0.255	−5.49	4.89	T
E96	0.488	>−3.74	<3.43	T
A97	0.0252	>−2.60	<1.00	D

[a] The methods used to follow the H/D-exchange reactions were as follows: T, TROSY; D, DMSO-QHX; H, direct HSQC measurement. For the log(k_{ex}/s^{-1}) values measured by the two methods (T and D), the average values are shown.

[b] The H/D-exchange rate was too fast to measure, and the lower limit of log(k_{ex}/s^{-1}) and the upper limit of log P_f are shown.

[c] The H/D-exchange rate was too slow to measure, and the upper limit of log(k_{ex}/s^{-1}) and the lower limit of log P_f are shown.

for the intrinsic chemical H/D-exchange reaction in the freely exposed state of the amide group and the k_{ex} measured by the H/D-exchange experiments, as

$$P_f = k_{int}/k_{ex} \quad (1)$$

The k_{int} values for the individual amide protons of GroES under the present conditions (pH* 6.5 and 7.5 at 25 °C) were evaluated from the amino acid sequence of GroES by the methods of Bai *et al.*[63] and Connelly *et al.*[64] The P_f values of the individual amide protons of GroES are included in Tables 1 and 2, and Figure 8 shows a protection profile that represents log P_f as a function of the residue number. We obtained the P_f values at pH* 6.5 for 28 amide protons (gray bars in Fig. 8), and the upper limits of P_f at pH* 6.5 for 61 amide protons (sticks and plus marks in Fig. 8). For the five amide protons of Leu6, Lys 13, Val40, Asp63, and Ile66, we could estimate the P_f values only from the exchange data at pH* 7.5 (blue bars in Fig. 8), because their exchange reactions were too slow at pH* 6.5.

Table 2. H/D-exchange parameters of GroES measured by TROSY at pH* 7.5 and 25 °C[a]

Residue	k_{int} (s^{-1})	$\log(k_{ex}/s^{-1})$	log P_f
L6	3.27	−6.20	6.72
I11	2.92	−5.94	6.41
V12	2.54	−6.03	6.44
K13	14.3	−5.70	6.85
V40	3.06	−5.91	6.39
L41	4.12	−6.47	7.09
K60	14.3	−5.75	6.91
D63	16.0	−5.86	7.06
I64	2.66	−5.58	6.00
V65	2.54	−6.14	6.54
I66	2.92	−6.20	6.67
L84	4.12	−5.07	5.68
I91	2.66	−6.07	6.50
V95	2.54	−4.43	4.84

[a] The parameter values for slowly exchanging protons measured by TROSY are shown.

To investigate the relationships between the protection profile in Fig. 8 and the secondary structure of GroES, we analyzed the X-ray crystallographic structure of the GroES portion of the GroEL/GroES/ADP complex (PDB code: 1AON)[49] by the method of Kabsch and Sander;[51] the PDB coordinates for stand-alone heptameric GroES are not yet published although its X-ray structure was reported.[48] The secondary structure of GroES consists of seven β-strands, several reverse turns, a 3_{10}-helix, and two loop regions (Fig. 1). The seven β-strands are labeled as A, B, C, D, E, F, and G in the order from the N-terminal to the C-terminal side, and they are shown at the top of Fig. 8. The highly protected amino acid residues with P_f values larger than 10^5 are mainly located in three β-strands (strands B, C, and D) that form the hydrophobic core of GroES, while the residues in the mobile loop (residues 17–34) are not highly protected (Fig. 8).

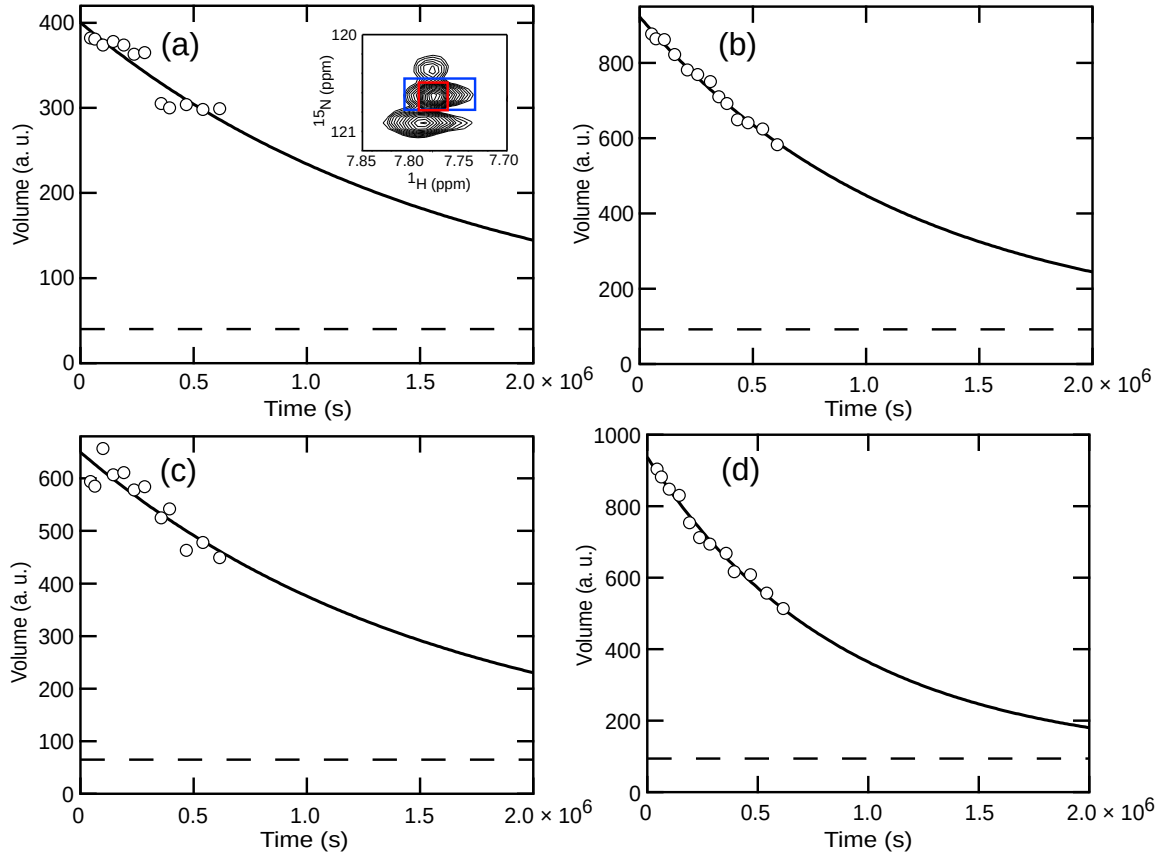

Fig. 7. The H/D-exchange progress curves of four unidentified amide protons, which are labeled a, b, c, and d in Fig. 3a, at pH* 7.5 and 25 °C. For cross-peak a, which appeared as a composite peak of the very slowly exchanging amide proton and the fast-exchanging I125 proton, we used the difference in the peak volume to extract solely the volume of the very slowly exchanging component by subtracting the volume enclosed by a red rectangle from the volume enclosed by a blue rectangle [inset of (a)]. The broken line in each panel is the peak volume at infinite time. The thick continuous lines are the theoretical exchange curves fitted to a single-exponential function [Eq. (13)] with k_{ex} values of 6.2×10^{-7} s^{-1} (a), 8.5×10^{-7} s^{-1} (b), 6.3×10^{-7} s^{-1} (c), and 1.1×10^{-6} s^{-1} (d).

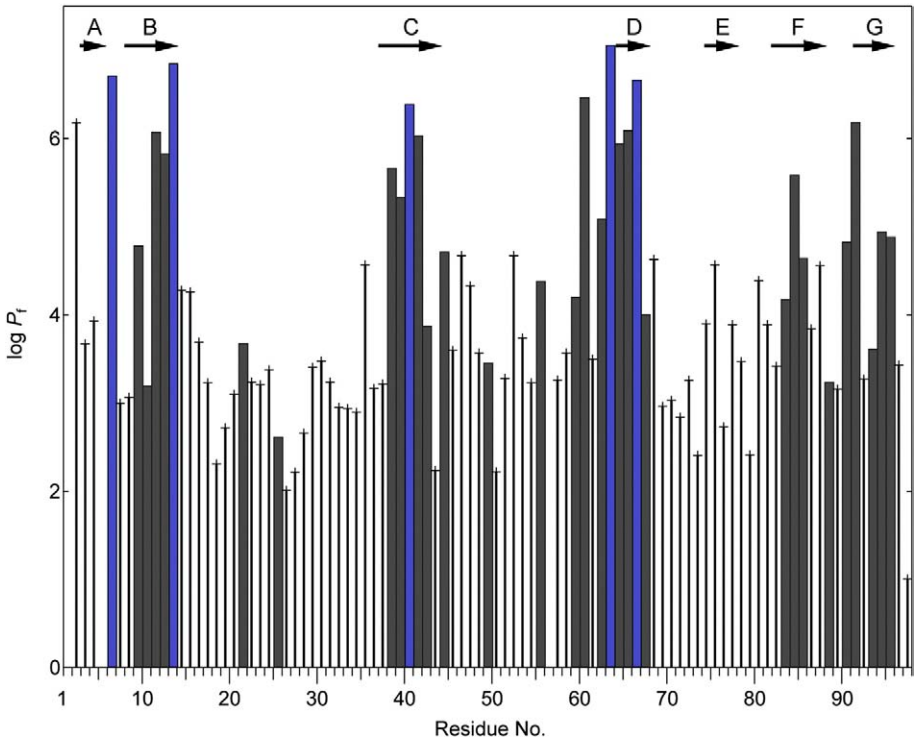

Fig. 8. The H/D-exchange protection profile represented by log P_f as a function of the residue number. The gray and blue bars indicate the P_f values at pH* 6.5 (28 amide protons) and pH* 7.5 (5 amide protons), respectively. The sticks and plus marks indicate the upper limits of P_f at pH* 6.5 (61 amide protons).

Discussion

We studied the H/D-exchange kinetics of individual amide protons of native heptameric GroES at pH* 6.5 and 7.5 at 25 °C. The use of the TROSY and DMSO-QHX techniques has made it possible to investigate the H/D-exchange behaviors of the individual identified amide protons of the protein supermolecular complex GroES, for which the conventional 2D NMR techniques could not give us much information. By using these techniques together with the direct HSQC experiments, we could quantitatively evaluate the k_{ex} values for 33 out of the 94 peptide amide protons and their P_f values, and for the remaining 61 residues, we obtained the lower and the upper limits of the k_{ex} and P_f values, respectively (Tables 1 and 2) (Fig. 8). The P_f values of the most highly protected amide protons were on the order of 10^6–10^7, and they were comparable in magnitude to those observed in typical small globular proteins, which have a molecular weight of 10,000–20,000.[61,65] However, the number of highly protected amide protons with P_f values larger than 10^6 was only 10 from Fig. 8, significantly smaller than the numbers reported for the small globular proteins, for example, more than 24 for barnase,[66] a 110-residue protein, and 36 for staphylococcal nuclease,[62] a 149-residue protein. Apparently, significant portions of GroES with P_f values less than 10^4 are not highly protected, although the most highly protected protons are protected to the same degree as observed in the small globular proteins.

The three-dimensional structure of GroES, the monomeric unit and the heptameric complex, are shown in Fig. 1a and b, respectively. The structure is presented in different colors according to the P_f values (red for $P_f < 10^4$, yellow for $10^4 \le P_f < 10^5$, cyan for $10^5 \le P_f < 10^6$, and blue for $10^6 \le P_f$). The structure of the GroES subunit consists of an irregular β-barrel formed by strands B, C, D, E and F; two loop regions; several reverse turns; a short 3_{10}-helix (residues 87–91); and the N- and C-terminal β-strands (strands A and G) that are located at the subunit–subunit interface (Fig. 1).[26,48–50] The highly protected amide protons with P_f values larger than 10^5 are located in four regions of the GroES molecule, that is, the major hydrophobic core formed mainly by three β-strands, B, C and D; a stable type-II β-turn formed by residues 60–63; the 3_{10}-helix of residues 87–91; and the subunit–subunit interface formed by Leu6 of one subunit and Ile91 of the preceding subunit. Strand A, strand E, and the two loop regions are not highly protected, and the P_f values for most residues are less than 10^4 (Fig. 8).

In the following, we discuss further details of the H/D-exchange behaviors of GroES. We also discuss the effective thermodynamic stability of GroES, evaluated from the P_f values of the most

highly protected amide protons,[61,65,67] and the relationship of the thermodynamic stability with the equilibrium unfolding parameters of GroES previously reported.[52–56,68]

The H/D-exchange behaviors

The most prevalent mechanism of the H/D-exchange protection is hydrogen bonding, and the hydrogen bond is thus broken before a protected amide proton is exchanged with a solvent deuteron.[62,69] In fact, all the highly protected amide protons ($P_f > 10^5$) except for those of Lys60 and Ile64 are hydrogen-bonded to a peptide carbonyl oxygen of the same chain or an adjacent chain.[26,48–50] The amide proton of Lys60 is hydrogen-bonded to the side-chain O^{δ} atom of Asp63. For the Ile64 amide proton, however, there is no possible acceptor group in the X-ray structural coordinates of GroES currently published in the PDB (PDB codes: 1AON, 1PCQ, 1PF9, 1SVT, and 1SX4).[26,49,50] A possible protection mechanism for the Ile64 amide proton is thus the hydrogen bonding to a water molecule that is strongly hydrated and integrated into the native protein structure,[62,69] although crystallographically determined water molecules are not observed around the GroES portion of the currently published PDB coordinates†.

The major hydrophobic core

The major hydrophobic core of GroES is organized by strands B, C, and D, and 10 residues in these β-strands (i.e., Ile11, Val12 and Lys13 in strand B; Gly38, Glu39, Val40, and Leu41 in strand C; and Ile64, Val65, and Ile66 in strand D) have a P_f value larger than 10^5. In addition to these residues, Leu84 of strand F and Ile91 of strand G are highly protected, with P_f values larger than 10^5, and their side chains are directly in contact with the major hydrophobic core, further stabilizing the hydrophobic core of GroES. The side chain of Ile91 also makes hydrophobic contacts with the side chain of Leu6 of the next adjacent chain, providing continuous hydrophobic interactions through the seven subunits of the GroES heptamer.[26,48–50]

Turns and a 3_{10}-helix

There are five turn conformations and one 3_{10}-helix in the monomeric unit of GroES, that is, five reverse turns of residues 6–9, 49–52, 60–63, 70–73, and 78–81, and a 3_{10}-helix of residues 87–91;[26,48–50] we ignored residues 17–34 of the mobile loop that is natively unfolded in free heptameric GroES. Among the residues of these turns and helix, Lys60, Gly62, and Asp63 in residues 60–63 (type-II β-turn) and Asp90 in residues 87–91 (3_{10}-helix) are highly protected, with P_f values larger than 10^5 (Tables 1 and 2; Fig. 8). Residues 60–63 are between the D strand and the roof hairpin (residues 44–58), and the Asp63 amide proton is hydrogen-bonded to the peptide carbonyl oxygen of Lys60. The amide proton of Lys60 is hydrogen-bonded to the side chain O^{δ} of Asp63, and the Gly62 amide proton is hydrogen-bonded to the peptide carbonyl oxygen of Val40 in the C strand, producing a β-bulge structure at the N-terminal end of strand D. Residues 87–91 form a two-turn 3_{10}-helix between strands F and G, and the Asp90 amide proton is hydrogen-bonded to the carbonyl oxygen of Ser87.

The subunit–subunit interface

The amide protons of Ile91 and Leu6 are very highly protected, with P_f values larger than 10^6 (Tables 1 and 2; Fig. 8), and the structure at the subunit–subunit interface is shown in Fig. 9. The Ile91 amide proton is hydrogen-bonded to the carbonyl oxygen of Glu88, forming a part of the 3_{10}-helix of residues 87–91. The side chain of Ile91 makes hydrophobic contacts with the Leu6 side chain of the next adjacent chain. The Leu6 amide proton is hydrogen-bonded to the Leu92 carbonyl oxygen of the preceding chain of GroES, and this hydrogen bonding and the hydrophobic contacts between the N- and C-terminal regions of the adjacent chains are the interactions that stabilize the subunit–subunit interface.[26,48–50] The importance of the C-terminal residues (Ile91 and Leu92)

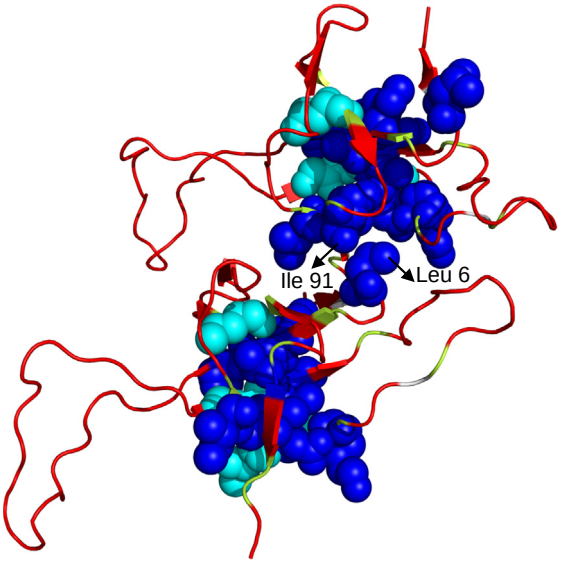

Fig. 9. The structure at the subunit–subunit interface of GroES (PDB code: 1AON). Two adjacent subunits of the GroES heptamer are shown, and the residues that have a P_f value larger than 10^5 are shown by a space-filling model. Leu6 and Ile91 are labeled. The structure is classified by different colors according to the P_f values as in Fig. 1. The figure was prepared using PyMOL (DeLano Scientific).

for the subunit–subunit interactions was also indicated by a C-terminal truncation experiment, in which the removal of the seven C-terminal residues prevented the heptamer formation of GroES.[70] Sakane *et al.*[55] also reported that the introduction of mutations that decreased hydrophobic contacts between the N- and C-terminal regions decreased the stability of the GroES heptamer.

Loop regions

There are two loop regions in the monomeric unit of GroES, that is, the mobile loop of residues 17–34 and the roof hairpin loop of residues 44–58. All the amide protons in the mobile loop region are unprotected, and their P_f values are less than 10^4 (Table 1). The mobile loop region is natively unfolded, and its amide proton signals are observed by 2D NMR with the chemical shift values expected for a random chain (Fig. 2a).[22] The results are consistent with the reported crystal structure of GroES, in which the mobile loop segment was disordered in the crystal structure in six out of the seven subunits.[48] The natively unfolded nature of the mobile loop is crucial for recognition by the chaperonin GroEL and the chaperonin cycling of the GroEL/GroES complex mediated by ATP hydrolysis.[23–25]

The roof hairpin of residues 44–58 is also not highly protected, with P_f values less than 10^5, and the amide proton of Asn51 that is located at the top of the roof hairpin was observed by the direct HSQC spectrum (Fig. 2a), indicating the flexible nature of the reverse turn (residues 49–52). The amide protons of two residues, Gly44 and Lys55, are, however, significantly protected, with P_f values of 4.9×10^4 and 2.4×10^4, respectively, indicating that the base and middle portions of the hairpin strands are not fully flexible. The amide protons of Gly44 and Lys55 are hydrogen-bonded to the carbonyl oxygen of Arg9 and Arg47, respectively.[26,48–50]

Effective thermodynamic stability of GroES

Among the 10 highly protected residues with P_f values larger than 10^6, 4 residues (i.e., Leu6, Lys13, Asp63, and Ile66) are the most highly protected, with an average P_f of 6.7×10^6 (Tables 1 and 2). These most highly protected amide protons are exchanged out through the global unfolding of GroES, and hence the P_f value is related to the effective thermodynamic stability, that is, the effective Gibbs free-energy change, ΔG_{eff}, of global unfolding, as described in the relation[61,65,67]

$$\Delta G_{eff} = RT \ln P_f \qquad (2)$$

The ΔG_{eff} thus obtained is 9.3 kcal/mol. However, the ΔG_{eff} of an oligomeric protein depends on the protein concentration, and for a heptameric protein, GroES, the dependence of ΔG_{eff} on the molar concentration, C, of the GroES monomer unit is given by[55,71]

$$\Delta G_{eff} = \frac{\Delta G^\circ}{7} + \frac{RT}{7} \ln\left(7 \cdot C^6\right) \qquad (3)$$

where ΔG° is the standard free-energy change that is independent of the protein concentration and $\Delta G^\circ/7$ is the ΔG° per monomer unit. The molar concentration C of GroES in *E. coli* cells is reported to be about 35 μM in monomer units,[58–60] and under a stress condition, the concentration may be 10 times higher (~350 μM).[58] The GroES concentration in the present study (300 μM) was within this range, and the ΔG_{eff} shown above (9.3 kcal/mol) is thus physiologically relevant. The ΔG_{eff} of 9.3 kcal/mol at 300 μM gives a ΔG° of 92.8 kcal/mol at 298.15 K, and at 35 μM, the ΔG_{eff} is thus estimated at 8.2 kcal/mol from Eq. (3) using this ΔG°. Although Eq. (3) is based on a simple two-state model of unfolding (see below),[71] the direct observation of the P_f values by the H/D exchange and the above estimates of ΔG_{eff} clearly indicate that the effective thermodynamic stability of GroES under physiological conditions is on the order of 8–10 kcal/mol. The effective thermodynamic stability of GroES is thus well designed so as to be comparable to the stability of typical small globular proteins, which is usually between 5 and 15 kcal/mol,[72] at physiological concentrations of GroES. An advantage of the H/D-exchange technique is that we can directly evaluate the effective thermodynamic stability of proteins and protein assemblies by Eq. (2) without any presumed models and extrapolations.

Global unfolding of GroES

The equilibrium unfolding transitions of GroES induced by denaturants (guanidine hydrochloride and urea) and by increasing temperature have been studied by a variety of techniques, including sedimentation equilibrium and velocity experiments,[52,68] intrinsic and extrinsic fluorescence spectroscopy,[52,54,56] circular dichroism spectroscopy,[53,56] differential scanning calorimetry,[53] size-exclusion chromatography,[54,55] and small-angle X-ray scattering.[57] The ΔG_{eff} can also be estimated from the equilibrium unfolding experiments, but unlike in the case of the H/D exchange, we need to extrapolate the free-energy change of unfolding obtained under unfolding conditions to the native physiological condition on the basis of a certain presumed model (two-state unfolding, three-state unfolding, or other) used for analysis of the experimental data. For a simple two-state unfolding of a monomeric protein, the linear–free-energy relationship with respect to the denaturant concentration has been well established,[73] and we can easily extrapolate the free-energy change to the native condition. However, for an oligomeric pro-

tein, the free-energy relationship is not that simple; the free energy also depends on the protein concentration [Eq. (3)]. Here, we thus compare the present results of the most stably protected amide protons ($P_f = 6.7 \times 10^6$ and ΔG_{eff} = 9.3 kcal/mol) and the known results of the equilibrium unfolding of GroES.[52–56,68]

Two-state model

The simplest model of the equilibrium unfolding of free heptameric GroES involves a two-state unfolding equilibrium between the heptameric native state, N_7, and the monomeric unfolded state, U, and the previous studies on the GroES unfolding often employed the two-state unfolding model.[52,53,56] The unfolding transition is thus represented by

$$N_7 \overset{K_U}{\rightleftarrows} 7U \tag{4}$$

where K_U is the equilibrium constant of unfolding, and K_U and the free-energy change, ΔG_U, of unfolding are given by

$$K_U = \frac{[U]^7}{[N_7]} \tag{5}$$

$$\Delta G_U = -(RT \ln K_U)/7 \tag{6}$$

where $[N_7]$ and [U] are the molar concentrations of N_7 and U, respectively, and ΔG_U is the free-energy change per mole of the GroES monomer. If we assume that the H/D-exchange rate in the U state is identical with the intrinsic chemical exchange rate k_{int} in the freely exposed state, the observed exchange rate constant k_{ex} based on the EX2 mechanism is given by[67]

$$k_{ex} = \frac{[U]}{7[N_7] + [U]} k_{int} \approx \frac{[U]}{7[N_7]} k_{int} = \frac{(K_U[N_7])^{1/7}}{7[N_7]} k_{int} = \frac{e^{-\Delta G_U/RT}[N_7]^{1/7}}{7[N_7]} k_{int} \tag{7}$$

where $[U] \ll 7[N_7]$, and the protection factor P_f is thus given by

$$P_f = \frac{7[N_7]}{(K_U[N_7])^{1/7}} = \frac{7[N_7]}{e^{-\Delta G_U/RT}[N_7]^{1/7}} \tag{8}$$

This equation is equivalent to Eq. (3), but here we calculate P_f values from the K_U or ΔG_U values previously reported and compare the calculated values with the P_f value (6.7×10^6) directly obtained by the H/D exchange.

Boudker *et al.*[53] analyzed the thermal unfolding and the unfolding of GroES by a denaturant, urea, by assuming the two-state model, and reported the ΔG_U values between 8 and 10.2 kcal/mol. Luke and Wittung-Stafshede[56] also carried out similar analyses of the equilibrium unfolding transitions of heptameric co-chaperonin proteins from 10 different species, including *E. coli* GroES, and reported the ΔG_U values between 7.9 and 8.6 kcal/mol for GroES. By assigning these values of ΔG_U and the molar concentration of N_7 ($[N_7] = 4.3 \times 10^{-5}$ M) in the present study to Eq. (8), we obtain a P_f value of $(0.99–38) \times 10^3$ (i.e., ΔG_{eff} = 4.1–6.2 kcal/mol). Apparently, the P_f value thus obtained is not consistent with the experimental P_f value (6.7×10^6) for the most highly protected amide protons, indicating that the simple two-state model of the GroES unfolding does not explain the H/D-exchange behavior of GroES. Zondlo *et al.*[68] carried out sedimentation equilibrium experiments for the GroES heptamer and obtained a dissociation constant of 1×10^{-38} M^6. If we assume the simple two-state unfolding model and assign this value to K_U in Eq. (8), we obtain a P_f of 3.4×10^2 (ΔG_{eff} = 3.5 kcal/mol), which is again much smaller than the experimental P_f value, indicating that the simple two-state model is not consistent with the present H/D-exchange results.

Three-state model

The Kawata group studied the guanidine hydrochloride-induced unfolding of GroES by 1-anilino-8-naphtalene sulfonate binding, intrinsic fluorescence spectroscopy, size-exclusion high-performance liquid chromatography analysis, and solution X-ray scattering,[54,55,57] and they found the presence of a monomeric folded intermediate of GroES during the unfolding transition. The unfolding of GroES thus occurs in at least two steps, (1) the dissociation of heptameric GroES into folded monomers and (2) the unfolding of the folded monomer, as

$$N_7 \overset{K_d}{\rightleftarrows} 7M \tag{9}$$

$$M \overset{K_u}{\rightleftarrows} U \tag{10}$$

where M represents the folded monomer and K_d and K_u are the dissociation constant of N_7 into seven monomers and the unfolding equilibrium constant between M and U, respectively. If we assume that the H/D-exchange reactions of the most stable protons occur only in the U state and that the exchange rate in the U state is identical with the k_{int}, the observed exchange rate constant k_{ex} is given by

$$k_{ex} \approx \frac{[U]}{7[N_7]k_{int}} = \frac{K_u(K_d[N_7])^{1/7}}{7[N_7]} k_{int} = \frac{e^{-\Delta G_u/RT} e^{-\Delta G_d/RT}[N_7]^{1/7}}{7[N_7]} k_{int} \tag{11}$$

where the concentrations of M and U are negligible compared with $7[N_7]$, and the protection factor P_f is thus given by

$$P_f = \frac{7[N_7]}{K_u(K_d[N_7])^{1/7}} = \frac{7[N_7]}{e^{-\Delta G_u/RT}e^{-\Delta G_d/RT}[N_7]^{1/7}} \quad (12)$$

According to Sakane *et al.*,[55] $K_d = 1.7 \times 10^{-37}$ M^6, and $K_u = 2.1 \times 10^{-2}$. By assigning these values to Eq. (12), we obtain a P_f value of 7.7×10^3 (ΔG_{eff} = 5.3 kcal/mol), which is again a few orders of magnitude smaller than the P_f value in the present study.

A possible molecular mechanism of the GroES unfolding

If the two-state and the three-state models of the GroES unfolding are not consistent with the H/D-exchange behavior of GroES, what kinds of molecular mechanisms of the GroES unfolding are possible? Although the results of the H/D-exchange experiments do not directly reveal the unfolding mechanism of GroES, the P_f values calculated from the previous two-state and three-state unfolding data were always a few orders of magnitude smaller than the P_f value (6.7×10^6) for the most highly protected amide protons in the present study, strongly suggesting that there are additional intermediates that were not taken into account in the previous models of GroES unfolding. We thus here hypothesize that such intermediates may be partially dissociated oligomeric species (hexamer, pentamer, tetramer, trimer, and dimer) of GroES, which were not considered in the previous models that assumed simultaneous dissociation from a heptamer to seven monomers [Eqs. (4) and (9)]. In support of this hypothesis, Sakane *et al.*[74] and Ikeda-Kobayashi *et al.*[75] recently reported that mechanical unfolding of covalently linked GroES showed a distinctive saw-tooth pattern that is typical for multimodular proteins, indicating the presence of such intermediates in which a subset of the subunits were detached and disrupted. The presence of such intermediates can reasonably explain the discrepancy between the previously reported equilibrium unfolding parameters and the P_f value in the present study, because the presence of the additional intermediates makes the unfolding transition less cooperative, leading to a smaller apparent unfolding free energy when analyzing the apparent unfolding transition by the simple two-state or three-state model. Nevertheless, further studies will be needed to elucidate the presence of such partially dissociated intermediates in wild-type GroES with no covalent links.

Another possibility that should also be considered for interpreting the discrepancy between the P_f values calculated from the previous unfolding data and those directly measured in the present H/D-exchange experiments is that the unfolded monomer retained some residual structure in certain regions, resulting in "hyper-protection" and P_f values in excess of the value calculated from the equilibrium unfolding data. In fact, the presence of residual structure in the unfolded state was reported in an H/D-exchange study of cytochrome *c*.[76] However, the protection factor in the unfolded state was reported to be on the order of 30,[76] much smaller than the protection factor, 2×10^2 to 2×10^4, expected from the above discrepancy between the P_f values. Furthermore, the residual structure in the unfolded state of cytochrome *c* arose from a cyclic structure stabilized by the heme thioether bridges and the His18 to heme coordination.[76] In GroES, there is no such covalent or coordination bond. A survey of the H/D-exchange literature found many proteins for which the slowest-exchanging amide protons when processed through Eq. (2) yield ΔG_{eff} values that closely match the unfolding free-energy values obtained by standard protein unfolding experiments,[61,65,67] further strengthening our conclusion that there are additional intermediates that were not taken into account in the previous models of GroES unfolding.

Materials and Methods

Materials

^{15}N-labeled and {^{13}C, ^{15}N}-double-labeled GroES proteins were expressed in *E. coli* host cells BL21(DE3) at 37 °C in M9 minimal medium using the expression plasmid pETESwild, which was a gift of Professor Y. Kawata (Tottori University).[57] The expression was induced with IPTG when the optical density of the culture medium was 0.6, and the cells were grown for 4–5 h after the induction. Perdeuterated and ^{15}N-labeled GroES ({D, ^{15}N}-GroES) was expressed in the *E. coli* cells grown in M9 minimal medium prepared in D_2O. The cells expressing the protein were collected by centrifugation and lysed by sonication in 50 mM Tris–HCl buffer (pH 7.5) that contained 2 mM ethylenediaminetetraacetic acid, 0.1 mg/mL DNase, 4 mM $MgCl_2$, and components in a tablet of complete protease inhibitor cocktail (Roche). The lysate was centrifuged at 17,000 rpm for 1 h at 4 °C, and the supernatant was heated at 80 °C for 20 min. After the heat treatment, the mixture was quickly cooled on ice for 30 min. To remove heat-denatured proteins, we centrifuged the heated mixture at 17,000 rpm for 40 min at 4 °C. The supernatant was precipitated with 55% saturation of ammonium sulfate overnight at 4 °C. The precipitate was collected by centrifugation at 17,000 rpm for 60 min at 4 °C and dissolved in Buffer A (50 mM Tris, pH 7.5, and 2 mM ethylenediaminetetraacetic acid). The soluble fraction of cell lysate was applied to a Sephacryl S-300 HR column equilibrated with Buffer A. The fractions containing GroES were pooled and further purified on a Q Sepharose FF

column (250 mL) equilibrated with Buffer A with a linear gradient of NaCl from 0.20 to 0.50 M.[8,57] The purified GroES was stored at −20 °C in Buffer A, which contained 15% (v/v) glycerol, to avoid degradation. The concentration of GroES was measured by UV absorption at 280 nm using an extinction coefficient, $E_{1cm}^{0.1\%}$ = 0.143, for GroES.[8]

The Zeba™ Spin Desalting Columns used in the DMSO-QHX experiments[47] were purchased from Thermo Scientific (Rockford, IL). DMSO-d_6 (99.9% D) and D_2O (99.9% D) were from Cambridge Isotope Laboratories (Andover, MA). All other chemicals were of guaranteed reagent grade.

H/D-exchange measurements

All the H/D-exchange experiments were carried out in Buffer B (25 mM phosphate and 20 mM KCl) at 25 °C, and the molar concentration of GroES (heptamer) was 43 μM. The H/D-exchange reaction was started by the 10-fold dilution of 430 μM GroES in the H_2O buffer into the D_2O buffer; the solution thus contained 10% H_2O and 90% D_2O. The pH* value was 6.5, and in the TROSY experiments, the measurements were also carried out at pH* 7.5. All NMR spectra were processed and analyzed by NMRPipe[77] and NMRView.[78]

TROSY experiments

{D, ^{15}N}-GroES was used in the TROSY experiments, and 2D ^{1}H–^{15}N TROSY spectra were recorded on a JEOL ECA 920-MHz NMR spectrometer every 2.5 h for 1 week during the H/D exchange at 25 °C. We acquired 32 transients for each of 256 t_1 points, and the sweep widths in t_1 and t_2 were 2799 and 14,988 Hz, respectively. The data acquisition for the first time point was started at approximately 3.3 h after the H/D exchange was started, and hence, the first time point was set at 4.6 h (=3.3 + 2.5/2 h).

Direct HSQC experiments

2D ^{1}H–^{15}N fast HSQC NMR spectra were recorded on a Bruker AVANCE 500-MHz NMR spectrometer every 12 min for 20 h during the H/D exchange at 25 °C. The ^{1}H flip angle was optimized at 75° for the fast HSQC measurement. The data acquisition for the first time point was started 14 min after the H/D exchange was started, and the first time point was set at 20 min (=14 + 12/2 min).

DMSO-QHX experiments

For the H/D-exchange experiments, a frozen stock GroES solution kept at −20 °C was thawed, and the buffer was exchanged for Buffer B (25 mM phosphate and 20 mM KCl at pH 6.5) using a PD-10 desalting column (GE Healthcare). After adjusting the GroES concentration to 430 μM in heptamers, the H/D-exchange reaction was started by 10-fold dilution of the GroES solution into Buffer B prepared in D_2O (pH* 6.5), giving the final GroES concentration of 43 μM (300 μM in monomer units). Immediately after the dilution, 1.0 mL of the reaction mixture was dispensed into each of 10–20 microtubes with a screw cap sealed by an O-ring to prevent water contamination, and the solutions in the tubes were incubated at 25.0 °C for H/D exchange. At each predetermined exchange time between 20 min and 10 days, the reaction mixture in a tube was taken, and the reaction was quenched in liquid nitrogen. The frozen mixtures were kept in a freezer at −85 °C until the medium exchange and the subsequent NMR measurement. For the NMR measurement, the frozen sample was first thawed at room temperature, and the medium containing Buffer B in 90% D_2O/10% H_2O was exchanged for the DMSO solution (95% DMSO-d_6/5% D_2O, pH* 5.0) by using a spin desalting column (Zeba™ Spin Desalting Column 89891, 5 mL; Thermo Scientific) as described by Chandak *et al.*[47] The ^{1}H–^{15}N HSQC spectrum of the protein in the DMSO solution was measured on a JEOL ECA 920-MHz NMR spectrometer at 25 °C. We acquired 16 transients for each of 256 t_1 points, and the sweep widths in t_1 and t_2 were 2426 and 13,827 Hz, respectively. The extent of H/D exchange at each time point was determined by the volume of each cross-peak in the HSQC spectrum.

To achieve the backbone resonance assignment of GroES in the DMSO solution, three-dimensional CBCA-CONH and HNCACB experiments were performed on a JEOL ECA 920-MHz spectrophotometer at 25 °C, and the ^{1}H, ^{13}C, and ^{15}N chemical shifts have been deposited in the BioMagResBank‡ under accession number BMRB-18949.

Data analysis

The observed kinetic exchange curves, given by the volumes [$Y(t)$] of cross-peaks in 2D NMR spectra as a function of the H/D-exchange time (t), were single exponential fitted to the equation

$$Y(t) = A \cdot e^{-k_{ex}} t + Y_\infty \qquad (13)$$

where A, k_{ex}, and Y_∞ are the kinetic amplitude, the observed H/D-exchange rate constant, and the final value of the peak volume, respectively. The fitting was performed by the IGOR Pro 6.2 software package (WaveMetrics). For the H/D-exchange reactions directly measured in the NMR probe (TROSY and direct HSQC), the Y_∞ value was expected to be 10% of the initial peak volume because the protein solution for the H/D exchange, being identical with the solution for the NMR measurement, contained 10% H_2O. For the DMSO-QHX experiments, however, the Y_∞ value was unpredictable because the H/D exchange was not completely quenched in the DMSO solution, so that an additional exchange occurred in the DMSO solution during the NMR measurement. In the DMSO-QHX experiments, we thus prepared a protein solution after complete exchange in Buffer B (90% D_2O/10% H_2O) by keeping the solution at 70 °C for 30 min and measured the NMR spectra of the completely exchanged protein in the DMSO solution to obtain Y_∞.

The H/D-exchange reaction of a peptide amide proton is generally described by a two-step process: (1) the opening process from the closed state (NH_{closed}), in which the amide proton is protected by hydrogen bonding, to the open state (NH_{open}), in which the amide proton is fully

accessible to solvent, and (2) the chemical H/D-exchange process by which the amide proton in NH_{open} is exchanged for a solvent deuteron with an intrinsic rate constant (k_{int}) for the chemical exchange of the amide proton, producing the amide-proton exchanged state ($ND_{exchanged}$), as[67]

$$NH_{closed} \underset{k_{cl}}{\overset{k_{op}}{\rightleftarrows}} NH_{open} \xrightarrow{k_{int}} ND_{exchanged} \quad (14)$$

where k_{op} and k_{cl} are rate constants for the opening and closing reactions, respectively, and under a native condition, $k_{cl} \gg k_{op}$. Under the present experimental conditions (pH* 6.5 or 7.5 and 25 °C), the H/D exchange is expected to occur in the EX2 regime (i.e., $k_{cl} > k_{int}$), and the observed H/D-exchange rate constant (k_{ex}) is given by[67]

$$k_{ex} = \frac{k_{op}}{k_{cl}} k_{int} = K_{op} k_{int} = k_{int}/P_f \quad (15)$$

where K_{op} is the equilibrium constant for the opening process, and it is identical with the inverse of P_f. For the most highly protected amide protons, K_{op} is equivalent to the equilibrium constant of global unfolding. The k_{int} values for individual amide protons of GroES were calculated from the amino acid sequence by the methods of Bai *et al.*[63] and Connelly *et al.*,[64] and we used the program SPHERE for the calculation of k_{int}; SPHERE is accessible through the internet§.

Acknowledgements

This study was supported by Grants-in-Aid for Scientific Research in Innovative Areas (project numbers: 20107004 and 20107009) from the Ministry of Education, Culture, Sports, Science and Technology of Japan. A part of this work was supported by the "Nanotechnology Platform Program" of the Ministry of Education, Culture, Sports, Science and Technology of Japan and the Joint Studies Program of the Institute for Molecular Science, Japan. We used the 920-MHz NMR instrument (JNM-ECA920) in the Research Center for Molecular Scale Nanoscience, Institute for Molecular Science. We thank Ms. Michiko Nakano (Institute for Molecular Science) for her technical assistance in the NMR measurements. We also thank Professor Yasushi Kawata (Tottori University) for providing us the expression plasmid (pETES-wild) and Professor John F. Hunt (Columbia University) for providing us the unpublished PDB coordinate of the refined X-ray structure of stand-alone GroES.

Received 17 January 2013;
Received in revised form 29 March 2013;
Accepted 5 April 2013
Available online 11 April 2013

Keywords:
molecular chaperone;
hydrogen/deuterium exchange;
protection factor;
protein supermolecular assembly;
transverse relaxation optimized spectroscopy

† In the PDB coordinate of the refined X-ray structure of stand-alone GroES (J. F. Hunt, personal communications), we find water molecules that are hydrogen-bonded to the Ile64 amide groups.
‡ http://www.bmrb.wisc.edu
§ http://www.fccc.edu/research/labs/roder/sphere/sphere.html

Present addresses: T. Nakamura, Fuji Pharma Co., Ltd., 1515 Tsujigado, Mizuhashi, Toyama 939-3515, Japan; K. Makabe, Graduate School of Science and Engineering, Yamagata University, 4-3-16 Jyonan, Yonezawa, Yamagata 992-8510, Japan; T. Takenaka, Institute for Chemical Research, Kyoto University, Gokasho Uji-city, Kyoto 611-0011, Japan.

Abbreviations used:
H/D, hydrogen/deuterium; 2D, two-dimensional; TROSY, transverse relaxation optimized spectroscopy, HSQC, heteronuclear single quantum coherence; DMSO, dimethylsulfoxide; DMSO-QHX, dimethylsulfoxide-quenched hydrogen/deuterium exchange; PDB, Protein Data Bank.

References

1. Fenton, W. A., Weissman, J. S. & Horwich, A. L. (1996). Putting a lid on protein folding: structure and function of the co-chaperonin GroES. *Chem. Biol.* **3**, 157–161.
2. Chaudhuri, T. K., Verrna, V. K. & Maheshwari, A. (2009). GroEL assisted folding of large polypeptide substrates in *Escherichia coli*: present scenario and assignments for the future. *Prog. Biophys. Mol. Biol.* **99**, 42–50.
3. Horwich, A. L. & Fenton, W. A. (2009). Chaperonin-mediated protein folding: using a central cavity to kinetically assist polypeptide chain folding. *Q. Rev. Biophys.* **42**, 83–116.
4. Thirumalai, D. & Lorimer, G. H. (2001). Chaperonin-mediated protein folding. *Annu. Rev. Biophys. Biomol. Struct.* **30**, 245–269.
5. Tang, Y. C., Chang, H. C., Roeben, A., Wischnewski, D., Wischnewski, N., Kerner, M. J. *et al.* (2006). Structural features of the GroEL–GroES nano-cage required for rapid folding of encapsulated protein. *Cell*, **125**, 903–914.
6. Katsumata, K., Okazaki, A. & Kuwajima, K. (1996). Effect of GroEL on the re-folding kinetics of α-lactalbumin. *J. Mol. Biol.* **258**, 827–838.
7. Okazaki, A., Katsumata, K. & Kuwajima, K. (1997). Hydrogen-exchange kinetics of reduced α-lactalbumin bound to the chaperonin GroEL. *J. Biochem. (Tokyo)*, **121**, 534–541.

8. Makio, T., Arai, M. & Kuwajima, K. (1999). Chaperonin-affected refolding of α-lactalbumin: effects of nucleotides and the co-chaperonin GroES. *J. Mol. Biol.* **293**, 125–137.
9. Cliff, M. J., Kad, N. M., Hay, N., Lund, P. A., Webb, M. R., Burston, S. G. & Clarke, A. R. (1999). A kinetic analysis of the nucleotide-induced allosteric transitions of GroEL. *J. Mol. Biol.* **293**, 667–684.
10. Inobe, T., Makio, T., Takasu-Ishikawa, E., Terada, T. P. & Kuwajima, K. (2001). Nucleotide binding to the chaperonin GroEL: non-cooperative binding of ATP analogs and ADP, and cooperative effect of ATP. *Biochim. Biophys. Acta*, **1545**, 160–173.
11. Inobe, T., Arai, M., Nakao, M., Ito, K., Kamagata, K., Makio, T. *et al.* (2003). Equilibrium and kinetics of the allosteric transition of GroEL studied by solution X-ray scattering and fluorescence spectroscopy. *J. Mol. Biol.* **327**, 183–191.
12. Inobe, T. & Kuwajima, K. (2004). Φ value analysis of an allosteric transition of GroEL based on a single-pathway model. *J. Mol. Biol.* **339**, 199–205.
13. Horovitz, A. & Willison, K. R. (2005). Allosteric regulation of chaperonins. *Curr. Opin. Struct. Biol.* **15**, 646–651.
14. Grason, J. P., Gresham, J. S. & Lorimer, G. H. (2008). Setting the chaperonin timer: a two-stroke, two-speed, protein machine. *Proc. Natl Acad. Sci. USA*, **105**, 17339–17344.
15. Inobe, T., Takahashi, K., Maki, K., Enoki, S., Kamagata, K., Kadooka, A. *et al.* (2008). Asymmetry of the GroEL–GroES complex under physiological conditions as revealed by small-angle X-ray scattering. *Biophys. J.* **94**, 1392–1402.
16. Hartl, F. U. & Hayer-Hartl, M. (2009). Converging concepts of protein folding in vitro and in vivo. *Nat. Struct. Mol. Biol.* **16**, 574–581.
17. Chakraborty, K., Chatila, M., Sinha, J., Shi, Q., Poschner, B. C., Sikor, M. *et al.* (2010). Chaperonin-catalyzed rescue of kinetically trapped states in protein folding. *Cell*, **142**, 112–122.
18. Motojima, F. & Yoshida, M. (2010). Polypeptide in the chaperonin cage partly protrudes out and then folds inside or escapes outside. *EMBO J.* **29**, 4008–4019.
19. Kovács, E., Sun, Z., Liu, H., Scott, D. J., Karsisiotis, A. I., Clarke, A. R. *et al.* (2010). Characterisation of a GroEL single-ring mutant that supports growth of *Escherichia coli* and has GroES-dependent ATPase activity. *J. Mol. Biol.* **396**, 1271–1283.
20. Chen, J., Makabe, K., Nakamura, T., Inobe, T. & Kuwajima, K. (2011). Dissecting a bimolecular process of $MgATP^{2-}$ binding to the chaperonin GroEL. *J. Mol. Biol.* **410**, 343–356.
21. Motojima, F., Motojima-Miyazaki, Y. & Yoshida, M. (2012). Revisiting the contribution of negative charges on the chaperonin cage wall to the acceleration of protein folding. *Proc. Natl Acad. Sci. USA*, **109**, 15740–15745.
22. Landry, S. J., Zeilstra-Ryalls, J., Fayet, O., Georgopoulos, C. & Gierasch, L. M. (1993). Characterization of a functionally important mobile domain of GroES. *Nature*, **364**, 255–258.
23. Landry, S. J., Taher, A., Georgopoulos, C. & Van der Vies, S. M. (1996). Interplay of structure and disorder in cochaperonin mobile loops. *Proc. Natl Acad. Sci. USA*, **93**, 11622–11627.
24. Shewmaker, F., Maskos, K., Simmerling, C. & Landry, S. J. (2001). The disordered mobile loop of GroES folds into a defined beta-hairpin upon binding GroEL. *J. Biol. Chem.* **276**, 31257–31264.
25. Shewmaker, F., Kerner, M. J., Hayer-Hartl, M., Klein, G., Georgopoulos, C. & Landry, S. J. (2004). A mobile loop order–disorder transition modulates the speed of chaperonin cycling. *Protein Sci.* **13**, 2139–2148.
26. Chaudhry, C., Horwich, A. L., Brunger, A. T. & Adams, P. D. (2004). Exploring the structural dynamics of the *E. coli* chaperonin GroEL using translation–libration–screw crystallographic refinement of intermediate states. *J. Mol. Biol.* **342**, 229–245.
27. Nishida, N., Motojima, F., Idota, M., Fujikawa, H., Yoshida, M., Shimada, I. & Kato, K. (2006). Probing dynamics and conformational change of the GroEL–GroES complex by ^{13}C NMR spectroscopy. *J. Biochem. (Tokyo)*, **140**, 591–598.
28. Hyeon, C., Lorimer, G. H. & Thirumalai, D. (2006). Dynamics of allosteric transitions in GroEL. *Proc. Natl Acad. Sci. USA*, **103**, 18939–18944.
29. Sameshima, T., Iizuka, R., Ueno, T., Wada, J., Aoki, M., Shimamoto, N. *et al.* (2010). Single-molecule study on the decay process of the football-shaped GroEL–GroES complex using zero-mode waveguides. *J. Biol. Chem.* **285**, 23159–23164.
30. Illingworth, M., Ramsey, A., Zheng, Z. & Chen, L. (2011). Stimulating the substrate folding activity of a single ring GroEL variant by modulating the cochaperonin GroES. *J. Biol. Chem.* **286**, 30401–30408.
31. Zhang, Q., Chen, J., Kuwajima, K., Zhang, H., Xian, F., Young, N. L. & Marshall, A. G. (2013). Nucleotide-induced conformational changes of tetradecameric GroEL mapped by hydrogen/deuterium exchange monitored by FT-ICR mass spectrometry. *Sci. Rep.* **3**, 1247.
32. Pervushin, K., Riek, R., Wider, G. & Wüthrich, K. (1997). Attenuated T2 relaxation by mutual cancellation of dipole–dipole coupling and chemical shift anisotropy indicates an avenue to NMR structures of very large biological macromolecules in solution. *Proc. Natl Acad. Sci. USA*, **94**, 12366–12371.
33. Fernandez, C. & Wider, G. (2003). TROSY in NMR studies of the structure and function of large biological macromolecules. *Curr. Opin. Struct. Biol.* **13**, 570–580.
34. Zhang, Y. Z., Paterson, Y. & Roder, H. (1995). Rapid amide proton exchange rates in peptides and proteins measured by solvent quenching and two-dimensional NMR. *Protein Sci.* **4**, 804–814.
35. Hoshino, M., Katou, H., Yamaguchi, K. I. & Goto, Y. (2007). Dimethylsulfoxide-quenched hydrogen/deuterium exchange method to study amyloid fibril structure. *Biochim. Biophys. Acta*, **1768**, 1886–1899.
36. Fiaux, J., Bertelsen, E. B., Horwich, A. L. & Wüthrich, K. (2002). NMR analysis of a 900K GroEL–GroES complex. *Nature*, **418**, 207–211.
37. Riek, R., Fiaux, J., Bertelsen, E. B., Horwich, A. L. & Wüthrich, K. (2002). Solution NMR techniques for large molecular and supramolecular structures. *J. Am. Chem. Soc.* **124**, 12144–12153.
38. Alexandrescu, A. T. (2001). An NMR-based quenched hydrogen exchange investigation of model amyloid fibrils formed by cold shock protein A. *Pac. Symp. Biocomput.* **6**, 67–78.

39. Hoshino, M., Katou, H., Hagihara, Y., Hasegawa, K., Naiki, H. & Goto, Y. (2002). Mapping the core of the β_2-microglobulin amyloid fibril by H/D exchange. *Nat. Struct. Biol.* **9**, 332–336.
40. Ippel, J. H., Olofsson, A., Schleucher, J., Lundgren, E. & Wijmenga, S. S. (2002). Probing solvent accessibility of amyloid fibrils by solution NMR spectroscopy. *Proc. Natl Acad. Sci. USA*, **99**, 8648–8653.
41. Kuwata, K., Matumoto, T., Cheng, H., Nagayama, K., James, T. L. & Roder, H. (2003). NMR-detected hydrogen exchange and molecular dynamics simulations provide structural insight into fibril formation of prion protein fragment 106–126. *Proc. Natl Acad. Sci. USA*, **100**, 14790–14795.
42. Yamaguchi, K. I., Katou, H., Hoshino, M., Hasegawa, K., Naiki, H. & Goto, Y. (2004). Core and heterogeneity of β_2-microglobulin amyloid fibrils as revealed by H/D exchange. *J. Mol. Biol.* **338**, 559–571.
43. Carulla, N., Caddy, G. L., Hall, D. R., Zurdo, J., Gairi, M., Feliz, M. *et al.* (2005). Molecular recycling within amyloid fibrils. *Nature*, **436**, 554–558.
44. Whittemore, N. A., Mishra, R., Kheterpal, I., Williams, A. D., Wetzel, R. & Serpersu, E. H. (2005). Hydrogen–deuterium (H/D) exchange mapping of $A\beta_{1-40}$ amyloid fibril secondary structure using nuclear magnetic resonance spectroscopy. *Biochemistry*, **44**, 4434–4441.
45. Dyson, H. J., Kostic, M., Liu, J. & Martinez-Yamout, M. A. (2008). Hydrogen–deuterium exchange strategy for delineation of contact sites in protein complexes. *FEBS Lett.* **582**, 1495–1500.
46. Chakraborty, S. & Hosur, R. V. (2011). NMR insights into the core of GED assembly by H/D exchange coupled with DMSO dissociation and analysis of the denatured state. *J. Mol. Biol.* **405**, 1202–1214.
47. Chandak, M. S., Nakamura, T., Takenaka, T., Chaudhuri, T. K., Yagi-Utsumi, M., Chen, J. *et al.* (2013). The use of spin desalting columns in DMSO-quenched H/D-exchange NMR experiments. *Protein Sci.* **22**, 486–491.
48. Hunt, J. F., Weaver, A. J., Landry, S. J., Gierasch, L. & Deisenhofer, J. (1996). The crystal structure of the GroES co-chaperonin at 2.8 Å resolution. *Nature*, **379**, 37–45.
49. Xu, Z. H., Horwich, A. L. & Sigler, P. B. (1997). The crystal structure of the asymmetric GroEL–GroES–$(ADP)_7$ chaperonin complex. *Nature*, **388**, 741–750.
50. Chaudhry, C., Farr, G. W., Todd, M. J., Rye, H. S., Brunger, A. T., Adams, P. D. *et al.* (2003). Role of the γ-phosphate of ATP in triggering protein folding by GroEL–GroES: function, structure and energetics. *EMBO J.* **22**, 4877–4887.
51. Kabsch, W. & Sander, C. (1983). Dictionary of protein secondary structure: pattern recognition of hydrogen-bonded and geometrical features. *Biopolymers*, **22**, 2577–2637.
52. Seale, J. W., Gorovits, B. M., Ybarra, J. & Horowitz, P. M. (1996). Reversible oligomerization and denaturation of the chaperonin GroES. *Biochemistry*, **35**, 4079–4083.
53. Boudker, O., Todd, M. J. & Freire, E. (1997). The structural stability of the co-chaperonin GroES. *J. Mol. Biol.* **272**, 770–779.
54. Higurashi, T., Nosaka, K., Mizobata, T., Nagai, J. & Kawata, Y. (1999). Unfolding and refolding of *Escherichia coli* chaperonin GroES is expressed by a three-state model. *J. Mol. Biol.* **291**, 703–713.
55. Sakane, I., Ikeda, M., Matsumoto, C., Higurashi, T., Inoue, K., Hongo, K. *et al.* (2004). Structural stability of oligomeric chaperonin 10: the role of two β-strands at the N and C termini in structural stabilization. *J. Mol. Biol.* **344**, 1123–1133.
56. Luke, K. & Wittung-Stafshede, P. (2006). Folding and assembly pathways of co-chaperonin proteins 10: origin of bacterial thermostability. *Arch. Biochem. Biophys.* **456**, 8–18.
57. Higurashi, T., Hiragi, Y., Ichimura, K., Seki, Y., Soda, K., Mizobata, T. & Kawata, Y. (2003). Structural stability and solution structure of chaperonin GroES heptamer studied by synchrotron small-angle X-ray scattering. *J. Mol. Biol.* **333**, 605–620.
58. Herendeen, S. L., VanBogelen, R. A. & Neidhardt, F. C. (1979). Levels of major proteins of *Escherichia coli* during growth at different temperatures. *J. Bacteriol.* **139**, 185–194.
59. Lorimer, G. H. (1996). A quantitative assessment of the role of chaperonin proteins in protein folding in vivo. *FASEB J.* **10**, 5–9.
60. Ellis, R. J. & Hartl, F. U. (1996). Protein folding in the cell: competing models of chaperonin function. *FASEB J.* **10**, 20–26.
61. Huyghues-Despointes, B. M., Pace, C. N., Englander, S. W. & Scholtz, J. M. (2001). Measuring the conformational stability of a protein by hydrogen exchange. *Methods Mol. Biol.* **168**, 69–92.
62. Skinner, J. J., Lim, W. K., Bedard, S., Black, B. E. & Englander, S. W. (2012). Protein hydrogen exchange: testing current models. *Protein Sci.* **21**, 987–995.
63. Bai, Y., Milne, J. S., Mayne, L. & Englander, S. W. (1993). Primary structure effects on peptide group hydrogen exchange. *Proteins*, **17**, 75–86.
64. Connelly, G. P., Bai, Y., Jeng, M. F. & Englander, S. W. (1993). Isotope effects in peptide group hydrogen exchange. *Proteins*, **17**, 87–92.
65. Huyghues-Despointes, B. M. P., Scholtz, J. M. & Pace, C. N. (1999). Protein conformational stabilities can be determined from hydrogen exchange rates. *Nat. Struct. Biol.* **6**, 910–912.
66. Perrett, S., Clarke, J., Hounslow, A. M. & Fersht, A. R. (1995). Relationship between equilibrium amide proton exchange behavior and the folding pathway of barnase. *Biochemistry*, **34**, 9288–9298.
67. Englander, S. W., Mayne, L. & Krishna, M. M. G. (2007). Protein folding and misfolding: mechanism and principles. *Q. Rev. Biophys.* **40**, 287–326.
68. Zondlo, J., Fisher, K. E., Lin, Z. L., Ducote, K. R. & Eisenstein, E. (1995). Monomer–heptamer equilibrium of the *Escherichia coli* chaperonin GroES. *Biochemistry*, **34**, 10334–10339.
69. Skinner, J. J., Lim, W. K., Bedard, S., Black, B. E. & Englander, S. W. (2012). Protein dynamics viewed by hydrogen exchange. *Protein Sci.* **21**, 996–1005.
70. Seale, J. W. & Horowitz, P. M. (1995). The C-terminal sequence of the chaperonin GroES is required for oligomerization. *J. Biol. Chem.* **270**, 30268–30270.

71. Park, C. & Marqusee, S. (2004). Analysis of the stability of multimeric proteins by effective Δ*G* and effective *m*-values. *Protein Sci.* **13**, 2553–2558.
72. Creighton, T. E. (1993). *Proteins: Structures and Molecular Properties*, Second Edition W. H. Freeman and Company, New York.
73. Santoro, M. M. & Bolen, D. W. (1992). A test of the linear extrapolation of unfolding free energy changes over an extended denaturant concentration range. *Biochemistry*, **31**, 4901–4907.
74. Sakane, I., Hongo, K., Mizobata, T. & Kawata, Y. (2009). Mechanical unfolding of covalently linked GroES: evidence of structural subunit intermediates. *Protein Sci.* **18**, 252–257.
75. Ikeda-Kobayashi, A., Taniguchi, Y., Brockwell, D. J., Paci, E. & Kawakami, M. (2012). Prying open single GroES ring complexes by force reveals cooperativity across domains. *Biophys. J.* **102**, 1961–1968.
76. Bai, Y., Sosnick, T. R., Mayne, L. & Englander, S. W. (1995). Protein folding intermediates: native-state hydrogen exchange. *Science*, **269**, 192–197.
77. Delaglio, F., Grzesiek, S., Vuister, G. W., Zhu, G., Pfeifer, J. & Bax, A. (1995). NMRPipe: a multi-dimensional spectral processing system based on UNIX pipes. *J. Biomol. NMR*, **6**, 277–293.
78. Johnson, B. A. & Blevins, R. A. (1994). NMR View: a computer program for the visualization and analysis of NMR data. *J. Biomol. NMR*, **4**, 603–614.